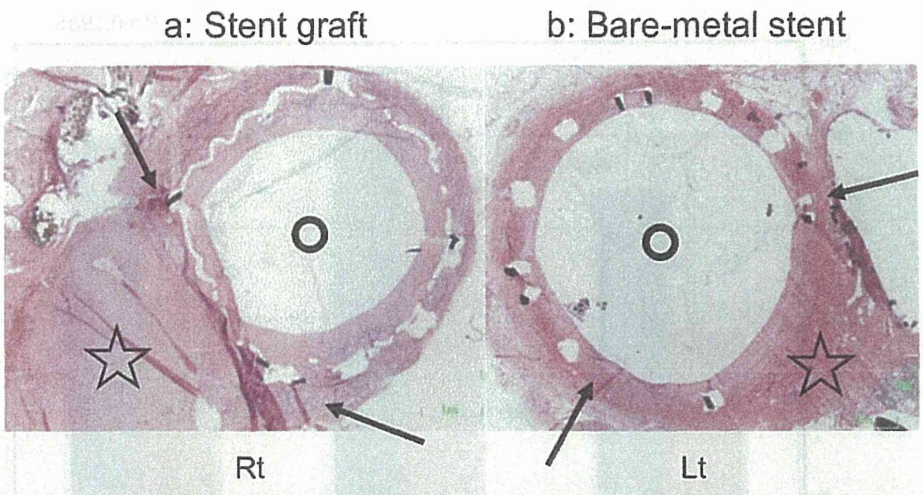


**Fig. 8.** Low-power cross-section photomicrograph of an aneurysm treated with a microporous, self-expanding stent graft and self-expanding bare-metal stent harvested at 6 and 12 months after implantation (hematoxylin-eosin staining). Organized thrombus formation within the aneurysm (asterisk) and mild intimal fibrocellular proliferation of the parent vessel wall (circle) is observed in both stent types. The neck of the aneurysm (arrows) corresponds to the arterial wall defect at the side-to-end anastomotic site of the carotid artery and the venous pouch.

[35]. The coiling of giant intracranial aneurysms may, in fact, aggravate the symptoms due to a mass effect [36], and fatal hemorrhage is known to occur after incomplete occlusion [37].

Stenting of cerebral aneurysms is based on the assumption that the metallic struts induce alterations in the blood flow dynamics within an aneurysm and therefore, induces and promotes thrombus formation and fibrosis within the residual aneurysmal lumen [17]. Intravascular stents are thus a potential treatment for aneurysms, especially large, fusiform aneurysms. The stents may pose lesser risk to the parent vessel and a lower risk of aneurysmal rupture than coils.

The long-term durability of the aneurysmal coil occlusion assisted by the new intracranial self-expandable stent (Neuroform; Stryker Neurovascular, Fermont, California, USA) has been reported to be stable after the first year in patients ($n = 41$) with intracranial wide-necked aneurysms (mean neck size, >5.33 mm) [7]. The procedure-related morbidity and mortality in 237 wide-neck intracranial aneurysms of 232 patients were 4.2 and 2.3%, respectively, mainly due to thromboembolism [5]. Further, in 36.1% (22 of 61) patients with complex aneurysms of a dome-to-neck ratio of <2 or a neck diameter >4 mm and that were inaccessible by conventional coil embolization, progressive occlusion by stent-assisted coiling was observed on angiographic follow-up imaging (mean, 19.42 months), possibly due to flow diversion [6]. The process of intimal hyperplasia can occur as early as 2 weeks to 6 months after stent deployment [38]. Therefore, the administration of concomitant anticoagulants (heparin and aspirin) is recommended during stenting [39]. With tantalum and stainless steel stents, the thickest neointimal build-up has been typically found at 8 weeks, decreasing by 26 weeks after the completion of the reparative process in the normal canine aorta, common iliac artery, and the coronary artery [40]. For stent-assisted coiling (Neuroform;

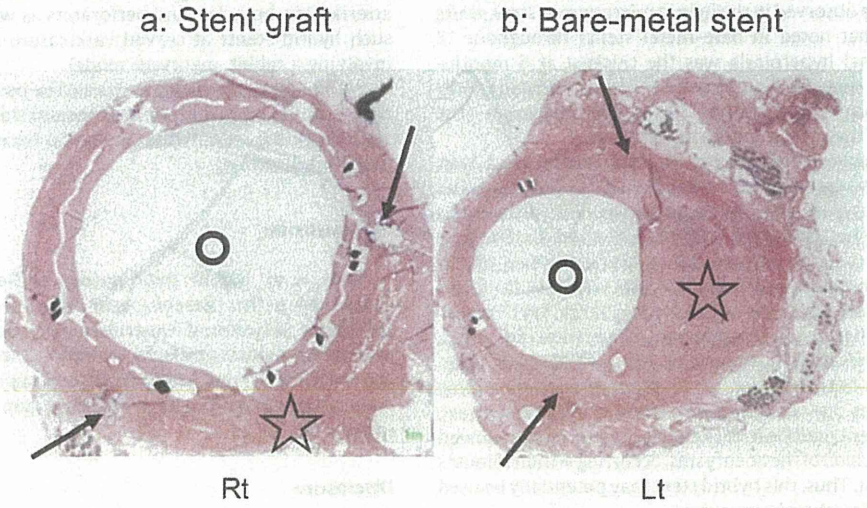


**Fig. 9.** Low-power cross-section photomicrograph of an aneurysm treated with a microporous, self-expanding stent graft and self-expanding bare-metal stent harvested at 6 and 12 months after implantation (hematoxylin-eosin staining). Organized thrombus formation within the aneurysm (asterisk) and mild intimal fibrocellular proliferation of the parent vessel wall (circle) is observed in both stent types. The neck of the aneurysm (arrows) corresponds to the arterial wall defect at the side-to-end anastomotic site of the carotid artery and the venous pouch.

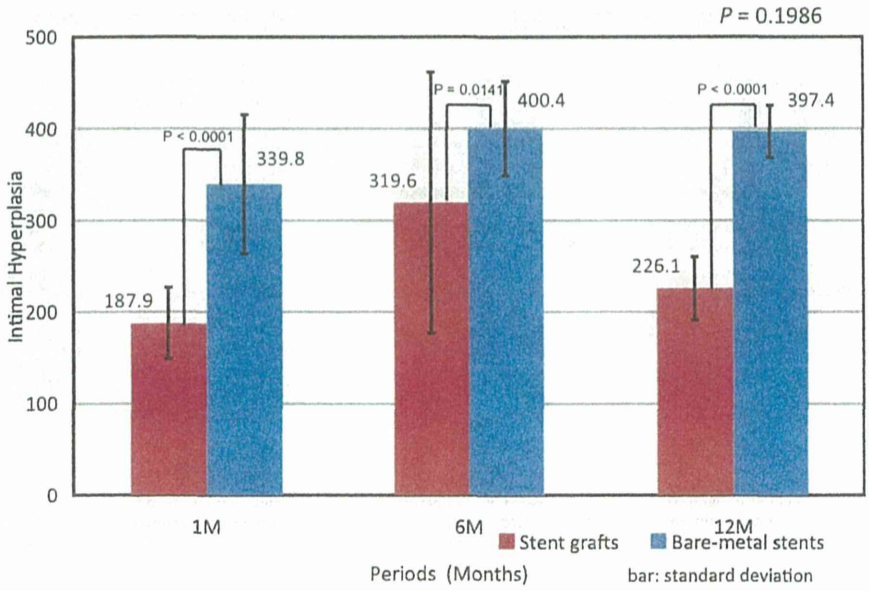


**Fig. 10.** Statistical analysis of intimal thickness. Repeated-measures ANOVA revealed that the intimal hyperplasia was lower in the group treated with microporous stent grafts than in the group treated with bare-metal stents, at all time points ($p < 0.0001$ at 1 month, $p = 0.0141$ at 6 months, and $p < 0.0001$ at 12 months). However, no statistically significant intragroup difference ($p = 0.1986$) was noted in the bare-metal stents or hybrid stent grafts across the different time points.

Stryker Neurovascular, or Enterprise; Cordis Neurovascular, Miami, Florida, USA), in-stent stenosis is reported to be uncommon, occurring in 2.5% (11 of 435) patients [41]. The porosity of 12.6% in microporous balloon expandable stents grafts was optimal for lesser intimal hyperplasia, when used for the occlusion of side-wall canine aneurysmal models [19,21,23]. According to this result, the porosity of 23.6% compared with the porosity of 12.6% was calculated and used in microporous self-expanding stent grafts [19]. Microporous self-expanding stent grafts with a porosity of 23.6% have been demonstrated to be associated with lesser intimal hyperplasia as compared to bare-metal stents with porosity of 86% or microporous stent grafts with porosity of 12.6%, at 1 month of aneurysmal occlusion [19]. Similarly, in the current study, the intimal hyperplasia observed in the hybrid microporous stent grafts was lesser than that noted in bare-metal stents throughout 12 months. The intimal hyperplasia was the thickest at 6 months, irrespective of the type of stent. Of course, the aneurysmal model used herein is not representative of saccular aneurysm (the commonest type), that occur at branching points.

Endovascular reconstruction with the PED represents a safe, durable, and curative treatment of selected wide-necked, large, and giant cerebral aneurysms [12]. The angiographic obliteration rates for PED were 91.2% (persistent filling, 8.4%) at 6 months and 94.6%, at up to 24 months, without retreatment in 251 aneurysms of 191 patients [13]. The morbidity and mortality rates were low, at 1% and 0.5%, respectively, with an event rate of 14.1% (27/191) [13]. Further occlusion occurred over a fairly long period (mean follow-up period, 5.9 months) after the initial incomplete occlusion of the aneurysms. Therefore, PED has been reported to be inappropriate for treating ruptured aneurysms due to continued endoleaks [12]. In contrast, the novel hybrid stent graft described in the present report showed almost instant occlusion of the aneurysms, occurring within minutes of stent deployment. Thus, this hybrid stent may potentially be used for the occlusion of ruptured aneurysms.

When the hybrid microporous stent graft was deployed as a balloon-expandable stent graft, all side-branches remained patent along with the occlusion of the aneurysms in elastase-induced rabbit carotid aneurysms for a 12-month period [42]. The present study demonstrated the successful long-term occlusion of canine carotid aneurysms, while maintaining the patency of the parent artery.

Stent grafts are thus a promising modality for the complete occlusion of aneurysms. An ideal covering for endovascular devices is expected to successfully occlude the aneurysm, preserve the arterial branches and perforators, and avoid parent vessel stenosis. To fulfill this need, we developed the hybrid self-expanding stent graft, described herein, for the treatment of large or giant cerebral aneurysms; this hybrid stent combines the merits of simple bare-metal stents and fully covered stents, while overcoming their individual disadvantages. We aim to evaluate the patency of arterial side-branches and perforators as well as the placement of such hybrid stents at curved vasculature sites in a future study involving a rabbit aneurysm model.

Although we have demonstrated the possibility of using hybrid stents for the occlusion of experimental side-wall aneurysms, stiff self-expanding stent struts remain an unresolved issue for use in the clinical setting.

## 5. Conclusion

The novel hybrid microporous self-expanding stent graft described in the present paper was useful for the successful complete occlusion of experimentally induced canine side-wall aneurysms, which persisted through 12 months. Further studies are required for evaluating the clinical application of these hybrid stent grafts in the treatment of large, giant, or dissecting carotid aneurysms.

## Disclosure

The authors report no conflict of interest concerning the materials or methods used in this study or the findings specified in this paper.

## References


[1] Chen SF, Kato Y, Subramanian B, Kumar A, Watabe T, Imizu S, et al. Retrograde suction decompression assisted clipping of large and giant cerebral aneurysms: our experience. Minim Invasive Neurosurg 2011;54:1–4.

[2] Li J, Lan ZG, Liu Y, He M, You C. Large and giant ventral paraclinoid carotid aneurysms; surgical techniques, complications and outcomes. Clin Neurol Neurosurg 2012;114:907–13.

[3] Ohtaki S, Mikami T, Iihoshi S, Miyata K, Nonaka T, Houkin K, et al. Strategy for the treatment of large-giant aneurysms in the cavernous portion of the internal carotid artery. No Shinkei Geka 2013;41:107–15.

[4] Gelfenbeyn M, Natarajan SK, Sekhar LN. Large distal anterior cerebral artery aneurysm treated with resection and interposition graft: case report. Neurosurgery 2009;64:E1008–9.

[5] Gao X, Liang G, Wei X, Hong Q. Complications and adverse events associated with Neuroform stent-assisted coiling of wide-neck intracranial aneurysms. Neurol Res 2011;33:841–52.

[6] Izar B, Rai A, Raghuram K, Rotruck J, Carpenter J. Comparison of devices used for stent-assisted coiling of intracranial aneurysms. PLoS One 2011;6:e224875.

[7] Sedat J, Chau Y, Mondot L, Vargas J, Szapiro J, Lonjon M. Endovascular occlusion of intracranial wide-necked aneurysms with stenting (Neuroform) and coiling: mid-term and long-term results. Neuroradiology 2009;51:401–9.

[8] Shapiro M, Becske T, Sahlein D, Babb J, Nelson PK. Stent-supported aneurysm coiling: a literature survey of treatment and follow-up. AJNR Am J Neuroradiol 33 2012;159–63.

[9] Krings T, Hans FJ, Möller-Hartmann W, BrunnA, Thiex R, Schmitz-Rode T, et al. Treatment of experimentally induced aneurysms with stents. Neurosurgery 2005;56:1347–60.

[10] Li MH, Li YD, Fang C, Gu BX, Cheng YS, Wang YL, et al. Endovascular treatment of giant or very large intracranial aneurysms with different modalities: analysis of 20 cases. Neuroradiology 2007;49:819–28.

[11] Fiorella D, Woo HH, Albuquerque FC, Nelson PK. Definitive reconstruction of circumferential fusiform intracranial aneurysms with the pipeline embolization device. Neurosurgery 2008;62:1115–21.

[12] Lylyk P, Miranda C, Ceratto R, Ferrario A, Scrivano E, Luna HR, et al. Curative endovascular reconstruction of cerebral aneurysms with the Pipeline embolization device: the Buenos Aires experience. Neurosurgery 2009;64:632–42.

[13] Saatci I, Yavuz K, Ozer C, Geyik S, Cekirge HS. Treatment of intracranial aneurysms using the Pipeline flow diverter embolization device: a single-center experience with long-term follow-up results. AJNR Am J Neuroradiol 33 2012;1436–46.

[14] Hassan T, Hamimi A. Successful endovascular management of brain aneurysms presenting with mass effect and cranial palsy. Neurosurg Rev 36 2013;87–97.

[15] Limaye US, Baheti A, Saraf R, Shriyastava M, Siddhartha W. Endovascular management of giant intracranial aneurysms of the posterior circulation. Neurol India 2012;60:597–603.

[16] Geremia G, Brack T, Brennecke L, Haklin M, Falter R. Occlusion of experimentally created fusiform aneurysms with porous metallic stents. AJNR Am J Neuroradiol 21 2000;739–45.

[17] Krings T, Busch B, Sellhaus B, Drexler AY, Bovi M, Hermanns-Sachweh B, et al. Long-term histological and scanning electron microscopy results of endovascular and operative treatments of experimentally induced aneurysms in the rabbit. Neurosurgery 2006;59:911–24.

[18] Waller BF, Orr CM, Pinkerton CA, Van Tassel JW, Pinto RP. Morphologic observation late after coronary balloon angioplasty: mechanisms of acute injury and relationship to restenosis. Radiology 1990;174:961–7.

[19] Nishi S, Nakayama Y, Ishibashi-Ueda H, Okamoto Y, Yoshida M. Development of microporous self-expanding stent graft grafts for treating cerebral aneurysms: designing micropores to control intimal hyperplasia. J Artif Organs 14 2011;348–56.

[20] Nishi S, Nakayama Y, Ishibashi-Ueda H, Okamoto Y, Kinoshita Y. High performance self-expanding stent graft; development and application to experimental aneurysms. J Artif Organs 12 2009;35–9.

[21] Nishi S, Nakayama Y, Ishibashi-Ueda H, Matsuda T. Occlusion of experimental aneurysms with heparin-loaded, microporous stent grafts. Neurosurgery 2003;53:1397–405.

[22] Flugelman MY, Virmani R, Leon MB, Bowman RL, Dichek DA. Genetically engineered endothelial cells remain adherent and viable after stent deployment and exposure to flow in vitro. Circ Res 1992;70:348–54.

[23] Nishi S, Nakayama Y, Ueda H, Ishikawa M, Matsuda T. A new stent graft with thin walled controlled micropored polymer covering. Intervent Neuroradiol 2000;6:175–80.

[24] Farrar DJ, Litwak P, Lawson JH, Ward RS, White KA, Robinson AJ, et al. In vivo evaluations of a new thrombo-resistant polyurethane for artificial heart blood pumps. J Thorac Cardiovasc Surg 1988;95:191–200.

[25] Giancario M, Mirko DO, Lacono C, Rozzanigo U, Serio G, Procacci C. Gastrointestinal artery stamp hemorrhage following pylorus-sparing whipple procedure: treatment with covered stents. Dig Surg 19 2002;237–40.

[26] Hue L, Greisler HP. Biomaterials in the development and future of vascular grafts. J Vasc Surg 37 2003;472–80.

[27] Kikumoto R, Tamao Y, Tezuka T, Tonomura S, Hara H, Ninomiya K, et al. Selective inhibition of thrombin by (2R, 4R)-4-methyl-1-(N2-(3-methyl-1,2,3,4-tetra-hydro-8quinolinyl) sulfonyl)-1-arginyl)) -2-piperidinecarboxylic acid. Biochemistry 23 1984;85–90.

[28] Kumada T, Abiko Y. Comparative study on heparin and a synthetic thrombin inhibitor no. 805 (MD-805*) in experimental antithrombin 3-deficient animals. Thromb Res 24 1981;285–98.

[29] Imanishi T, Arita M, Hamada M, Tomobuchi Y, Hano T, Nishio I. Effects of locally administration of argatroban using a hydrogel-coated balloon catheter on intimal thickening induced by balloon injury. Jpn Circ J 1997;61:256–62.

[30] Richey T, Iwata H, Oowaki H, Uchida E, Matsuda S, Ikada Y. Surface modification of polyurethane balloon catheters for local drug delivery. Biomaterials 21 2000;1057–65.

[31] Molyneux A, Kerr R, Stratton I, Sandercock P, Clarke M, Shrimpton J, et al. International Subarachnoid Aneurysm Trial (ISAT) Collaborative Group International Subarachnoid Trial (ISAT) of neurosurgical clipping versus endovascular coiling in 2143 patients with ruptured intracranial aneurysms; a randomized trial. Lancet 2002;360:1267–74.

[32] Gruber A, Killer M, Bavinzski G, Richling B. Clinical and angiographic results of endovascular coiling treatment of giant and very large intracranial aneurysms: a 7-year, single-center experience. Neurosurgery 1999;45:793–800.

[33] Fiorella D, Albuquerque FC, McDougall CG. Durability of aneurysm embolization with matrix detachable coils. Neurosurgery 2006;58:51–9.

[34] Khan SH, Nichols C, Depowell JJ, Abruzzo TA, Ringer AJ. Comparison of coil types in aneurysm recurrence. Clin Neurol Neurosurg 2012;114(1):12–6.

[35] Chalouhi N, Tjoumakaris S, Gonzalez LF, Dumont AS, Starke RM, Hasa D, et al. Coiling of large and giant aneurysms; complications and long-term results of 334 cases. AJNR Am J Neuroraiol 2013;(August)334 Epub ahead of print.

[36] Malisch TW, Guglielmi G, Vinuela F, Duckwiler G, Gobin YP, Martin NA, et al. Intracranial aneurysms treated with Guglielmi detachable coils: midterm clinical results in a consecutive series of 100 patients. J Neurosurg 1997;87:176–83.

[37] Ross IB, Weil A, Piotin M, Moret J. Endovascular treatment of distally located giant aneurysms. Neurosurgery 2008;62:1354–60.

[38] Mehta B, Burke T, Kole M, Bydon A, Seyfried D, Malik G. Stent-within-stent technique for the treatment of dissecting vertebral artery aneurysm. AJNR Am J Neuroradiol 2003;24:1814–8.

[39] Sigwart U, Puel J, Mirkovitch V, Joffre F, Kappenberger L. Intravascular stents to prevent occlusion and restenosis after transluminal angioplasty. N Engl J Med 1987;316:701–6.

[40] Barth KH, Virmani R, Strecker EP, Savin MA, Lindisch D, Matsumoto AH, et al. Flexible tantalum stents implanted in aortas and iliac arteries; effects in normal canines. Radiology 1990;175:91–6.

[41] Chalouhi N, Drueding R, Starke RM, Jabbour P, Dumont AS, Gonzalez LF, et al. In-stent stenosis following stent-assisted coiling: incidence, predictors and clinical outcomes of 435 cases. Neurosurgery 2013;72:390–6.

[42] Nishi S, Nakayama Y, Ishibashi-Ueda H, Yoshida M, Yonetani H. Treatment of rabbit carotid aneurysms by hybrid stents (microporous thin polyurethane-covered stents): preservation of side-branches. J Biomater Appl 2014(January) (Epub ahead of print).

Society For Biomaterials

# Basic study of soft tissue augmentation by adipose-inductive biomaterial

**Masaki Yazawa,[1] Taisuke Mori,[2] Yasuhide Nakayama,[3] Kazuo Kishi[1]**

[1]Department of Plastic and Reconstructive Surgery, School of Medicine, Keio University, Tokyo, Japan
[2]Department of Pathology, National Cancer Center Laboratory, Tokyo, Japan
[3]Division of Medical Engineering and Materials, National Cerebral and Cardiovascular Center Research Institute, Osaka, Japan

Received 19 December 2013; revised 25 February 2014; accepted 12 April 2014
Published online 25 April 2014 in Wiley Online Library (wileyonlinelibrary.com). DOI: 10.1002/jbm.b.33180

**Abstract:** Reconstructive surgery for tumor resection, trauma, and congenital anomaly involves volume augmentation with autologous tissue transfer. However, a healthy region is damaged as a donor site, and the autologous tissue is transferred like a patchwork to the recipient site. We have attempted to induce adipogenesis activity in artificial biomaterial that is injectable with an injection needle for soft tissue augmentation. First of all, the optimal dose of pioglitazone hydrochloride was examined with adipo-precursor cells in terms of the proliferator-activated receptor-γ mRNA expression levels affected by reagent *in vitro*. Then, salmon collagen with pioglitazone was adjusted in terms of the dose and the salmon collagen was injected into mouse back using an injection needle *in vivo*. At 4 weeks after implantation, the pioglitazone collagen gel was substituted by mature adipocytes in comparison with the case for control collagen gel without pioglitazone. These results are indicative of the possibility of promoting adipogenesis using collagen with pioglitazone as an adipose-inductive substance. © 2014 Wiley Periodicals, Inc. J Biomed Mater Res Part B: Appl Biomater, 103B: 92–96, 2015.

**Key Words:** adipose, biomaterial, augmentation, soft tissue

**How to cite this article:** Yazawa M, Mori T, Nakayama Y, Kishi K. 2015. Basic study of soft tissue augmentation by adipose-inductive biomaterial. J Biomed Mater Res Part B 2015:103B:92–96.

## INTRODUCTION

In recent years, advances in medicine have spectacularly improved the survival rate in tumor resection, trauma, and congenital anomaly. However, some patients cannot obtain a sufficient quality of life because of poor appearance after treatments. At present, reconstructive surgery for tumor resection, trauma, and congenital anomaly involves volume augmentation with autologous tissue transfer. However, a healthy region is damaged as a donor site, and the autologous tissue is transferred like a patchwork to the recipient site. Therefore, the quality of life of patients is not improved sufficiently.

Now, a new tissue transfer method without the problems at donor and recipient sites is required. We have attempted to induce adipogenesis activity in artificial biomaterial that is injectable using an injection needle, with the goal of its clinical application. To achieve this, pioglitazone hydrochloride was selected because it has been applied in clinical treatment as a diabetic medicine and has been reported to induce adipogenesis via peroxisome proliferator-activated receptor-γ (PPAR-γ).[1,2]

As an injectable artificial biomaterial, salmon collagen was selected because it is clinically available and should work as a scaffold for adipose tissue by ligand protein interaction.[3–7]

First of all, the optimal dose of pioglitazone was examined. Then, salmon collagen with pioglitazone was adjusted in terms of the dose and the salmon collagen was injected using an injection needle *in vivo*. Finally, adipogenesis at the recipient site was estimated in terms of the function of the artificial material as a transplant bed for adipogenesis.

## MATERIALS AND METHODS

### Animal care

The experimental procedure was authorized and reviewed by the Keio University Experimental Animal Center Committee (Approval no. 10256(0)).

Forty C3H/He/N mice (8 weeks, male, body weight 25–30 g; purchased from Charles River Laboratories Japan Inc., Tokyo, Japan) were used in the current study. All surgeries were performed in an animal-operating suite at the university.

### Histological analysis

All tissue samples were obtained by mouse experiment and were fixed in 10% formalin and embedded in paraffin.

**Correspondence to:** M. Yazawa (e-mail: prsyazawa@gmail.com)
Contract grant sponsor: Japan Society for the Promotion of Science; contract grant number: KAKENHI 23792059

Subcutaneous transplanted materials were histologically evaluated.

### Adipose precursor isolation and cell culture

To study adipo-precursor cells in terms of their PPAR-γ mRNA expression levels induced by the reagent *in vitro*, we isolated cells from the subcutaneous fat pad tissue of mice at a lower-back site. Briefly, tissue was minced and incubated for 1 h at 37°C in a rotary shaking bath at 100 rpm in digestion buffer containing collagenase (5 mg/mL) before being filtered through a 400-μm nylon mesh. The adipo-precursor cells were washed twice with serum-free Dulbecco's modified Eagle's medium (DMEM) (pH 7.4, 10 n*M* 4-(2-hydroxyethyl)-1-piperazineethanesulfonic acid (HEPES), containing penicillin/streptomycin) and incubated at 37°C under sterile tissue culture conditions. The adipo-precursor cells were expanded in bulk culture to avoid any biases resulting from cloning, and subjected to further analysis.

For cell proliferation assay, we used "passage two" adipose precursor cells as this would eliminate the hematocytes. About $1 \times 10^5$ cells were seeded into six cell culture plates in triplicate and counted at 14 days. For the induction of PPAR-γ mRNA expression, 100, 10, and 1 μ*M* pioglitazone (pioglitazone hydrochloride, Tokyo Chemical Industry, Tokyo, Japan), 200, 20, and 2 ng/mL insulin-like growth factor (IGF) 1 (PeproTech, NJ), and 200, 20, and 2 ng/mL IGF2 (PeproTech, NJ) were each added to the culture medium.

### Quantitative reverse transcription PCR

Total RNAs were extracted with the RNeasy Mini kit (Qiagen, Valencia, CA) and reverse-transcribed using the SuperScript III RT-PCR system (Invitrogen, Carlsbad, CA) according to the manufacturer's protocol. We did not change the media for 2 weeks for the induction of adipocytes. One microliter of cDNA sample was amplified by PCR gene-specific primers. For quantitative RT-PCR (qRT-PCR), reactions were performed in triplicate using Fast Start Universal Probe Master (Roche Applied Science, Penzberg, Germany). The primer sets were as follows: for mouse PPAR-γ: 5′-ATCATCTACACGATGCTGGCC-3′ (forward), 5′-CTCCCTGGTCATGAATCCTTG-3′ (reverse); and for GAPDH: 5′-CACCATGGAGAAGGCCGGGG-3′ (forward), 5′-GACG GACACATTGGGGGTAG-3′ (reverse).

### Statistical analysis

Data are expressed as mean ± SE (standard error). The relative mRNA expression levels were compared using unpaired *t*-test and all statistical analyses were performed using Statcel software (OSM, Japan). The results were judged significant at $p < 0.05$.

### Adipogenesis by artificial biomaterial with pioglitazone *in vivo*

Nine C3H/He/N mice were used and maintained under specific pathogen-free conditions throughout this experiment. The optimal dose of pioglitazone was determined to be 10 μ*M* by previous cell proliferation assays. About 0.5% salmon collagen particles with and without pioglitazone (10 μ*M*) (0.9 g each, both from IHARA & Co., Ltd., Japan) were produced as follows. The salmon atelocollagen W/O (water in oil) emulsion was made by span20 (sorbitan monolaurate). The salmon collagen crosslinked by EDC (1-ethyl-3-(dimethylaminopropyl) carbodiimide hydrochloride) was settled down as particles to the water phase of 50% (vol/vol) EtOH. Dried particles were mixed with pioglitazone (10 μ*M*) solution and aspirated. The collagen particles with and without pioglitazone were dispersed in 0.9 mL of saline. About 0.1 mL of collagen gel with and without pioglitazone was injected under bilateral dorsal skin layer using an 18-G injection needle. The mice were then sacrificed and evaluated pathologically at 1, 2, and 4 weeks after operation. Three replicate samples were performed for each test. In addition, the area of adipose tissue was calculated in the histologic sections using software (Photoshop 7.0, Adobe, USA).

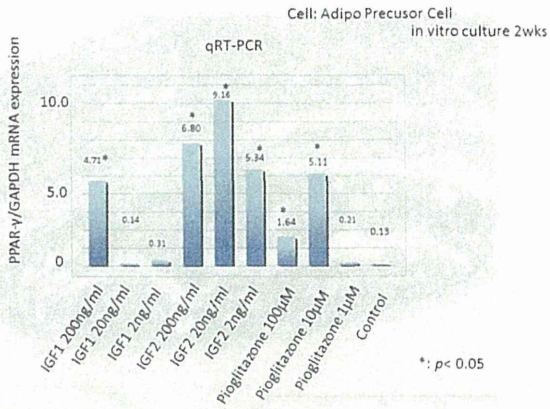


**FIGURE 1.** Pioglitazone and IGFs up-regulated PPAR-γ mRNA levels in mouse adipo-precursor cells. Mouse adipo-precursor cells were incubated for 2 weeks with pioglitazone, IGF1, or IGF2 at the indicated doses, and PPAR-γ mRNA levels were determined by qRT-PCR. *$p < 0.05$ versus control. [Color figure can be viewed in the online issue, which is available at wileyonlinelibrary.com.]

## RESULT

### Pioglitazone and IGFs up-regulated PPAR-γ mRNA levels

PPAR-γ is considered to be one of the master regulators of adipocyte differentiation (Figure 1).[8] To evaluate the potential effects of pioglitazone and IGFs on PPAR-γ expression, we exposed mouse adipo-precursor cells to these substances for 2 weeks and performed qRT-PCR. As shown in Figure 1, the dose responses of the expression level of PPAR-γ mRNA with pioglitazone, IGF1, IGF2, and control (without any reagent) were quantitatively analyzed in cultured cells. The PPAR-γ expression levels were efficiently up-regulated dose-dependently by all reagents, whereas 100 μ*M* pioglitazone caused cell toxicity (mean relative levels: pioglitazone 1 μ*M* vs. 10 μ*M* vs. 100 μ*M* = 0.21 vs. 5.11 vs. 1.64; mean relative levels: IGF1 2 ng/mL vs. 20 ng/mL vs. 200 ng/mL = 0.31 vs. 0.14 vs. 4.71; mean relative levels: IGF2 2 ng/mL vs. 20 ng/mL vs. 200 ng/mL = 5.34 vs. 9.16 vs. 6.80). The effective induction abilities of PPAR-γ by pioglitazone

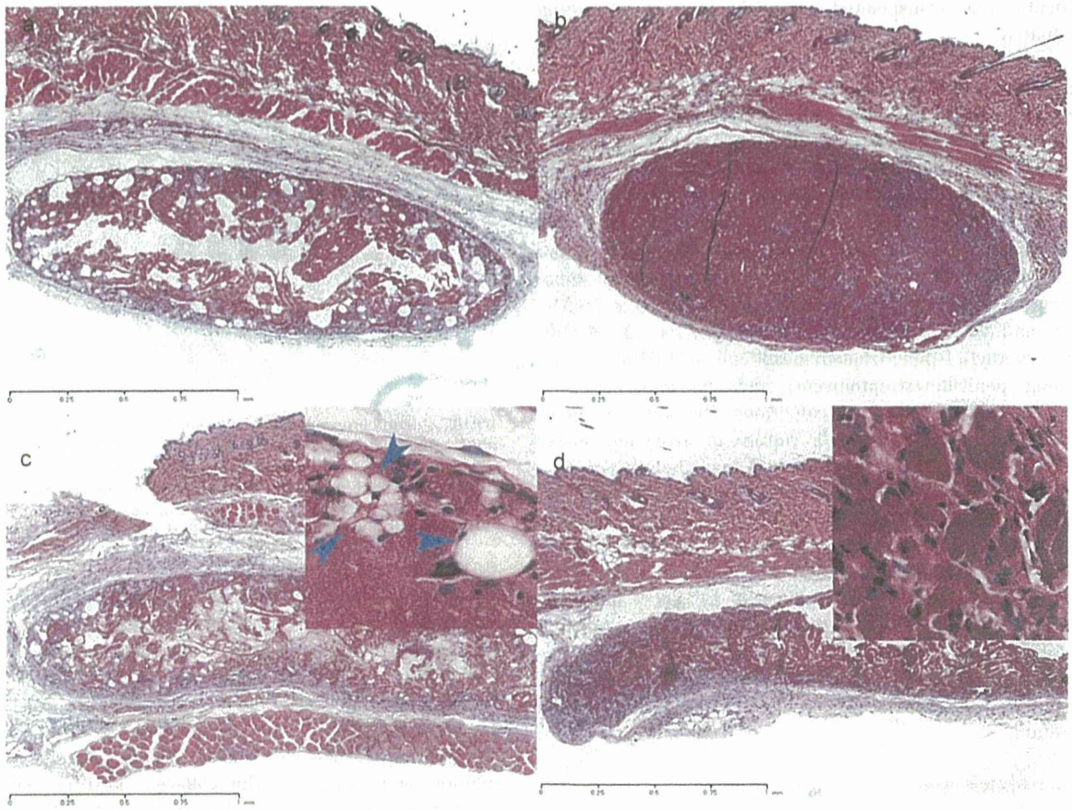


FIGURE 2. Photomicrographs of sections from implanted collagen gel after 1 week and 4 weeks. At 1 week after implantation, both the collagen gels were observed without any immune elimination (a, b). At 4 weeks after implantation, the pioglitazone collagen gel (c) was substituted by mature adipocytes (arrow heads) in comparison with the case for control gel (d). (a, c) Collagen gel with pioglitazone at 10 $\mu M$; (b, d) collagen gel only (H&E staining, original magnification 100× and insets 400×). [Color figure can be viewed in the online issue, which is available at wileyonlinelibrary.com.]

and IGFs were not significantly different from the control ($n = 3$; $p > 0.05$).

### Quantification of induced adipose tissue *in vivo*

We evaluated the time course of the areas of adipose tissue induced by pioglitazone/collagen gel (induced group) that was comprised of mature adipose cells relative to the total implanted gel area (Figures 2 and 3). For mature adipose cells observed at the edge of the pioglitazone/collagen gel after one week of implantation, the average area percentage was 4.29%. In contrast, few adipose cells were observed in the collagen gels without pioglitazone (control group); the average area percentage was 0.343%. The collagen gels without pioglitazone as a control began to degrade without the induction of adipose cells from 2 weeks. In contrast, in the collagen gels with pioglitazone as an induced group, the replacement of adipose cells was observed. The induced group had higher proportions of adipose cells in the gels in a time-dependent manner after 2 weeks and 4 weeks. The average area percentages were 5.36% in the induced group and 0.394% in the control group after 2 weeks. They were 17.7% in the induced group and 1.20% in the control group after 4 weeks, as shown in Figure 3. There were statistically significant differences between the induced group and the control group ($p < 0.05$).

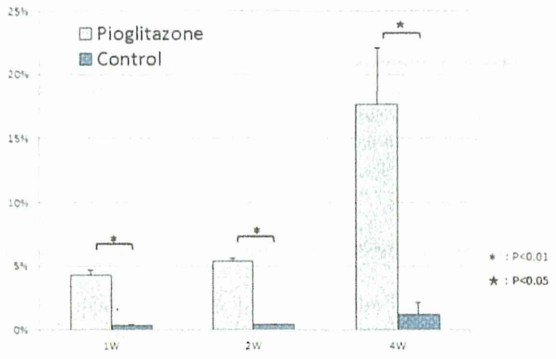


FIGURE 3. Area percentages of induced adipose tissue *in vivo*. [Color figure can be viewed in the online issue, which is available at wileyonlinelibrary.com.]

## DISCUSSION

In the field of reconstructive surgery, operative techniques for autologous tissue transfer and medical technology in artificial materials have improved. To obtain autologous tissue, however, there is still a need for a donor site in a healthy body area, which is sutured to the recipient site like a patchwork for volume augmentation. This is not ideal in terms of patient satisfaction. In the case of hard tissue, artificial bone has already been developed into block and liquid types with processability for clinical applications, while liquid artificial bone is injectable with an injection syringe. On the other hand, in the case of soft tissue, various methods have been reported for fat augmentation.[9,10] However, these reports require a healthy donor site and the obtained results have not always been stable in the long-term. For example, fat tissue is taken from a small incision at a healthy area of a patient by suction and the fat tissue is injected into the recipient area of the patient using a syringe.[11] Besides, Kimura et al. reported a combination method involving autologous fat cells and artificial material.[12] The volume rate of grafted fat tissues is, nevertheless, unstable and unpredictable, with most of the volume being absorbed as time passes. These lines of evidence indicate the possibility of repetitive operations and overdose of fat grafting. These conventional methods for autologous fat grafting always need a healthy donor site and the patient is subjected to an invasive burden by repetitive operations. As such, the development of a new approach for soft tissue augmentation has long been anticipated internationally.

In this study, our ideas were based on our previous report that mesenchymal stromal cells induced adipocytes.[13] For an adjunct to artificial biomaterial, pioglitazone hydrochloride was focused on as a substance for adipose induction and maintenance.[14–16] Youm et al. reported that pioglitazone induces ectopic adipogenesis via PPAR-γ.[1] Pioglitazone hydrochloride is already used for diabetic patients in clinical applications.

Therefore, the optimal concentration of pioglitazone for the efficient induction and promotion of adipose tissue was examined. The mRNA levels of PPAR-γ, which is considered to be one of the master regulators of adipocyte differentiation,[17] were examined by qRT-PCR *in vitro*. IGF1 and IGF2 were used for comparison. The concentrations of each substance, pioglitazone, IGF1, and IGF2, were set at three levels using examples from previous reports.[18,19] It was found that 10 μ*M* pioglitazone was associated with a significantly high PPAR-γ mRNA level for adipo-precursor cells (Av. 5.11, $p < 0.05$). In addition, 100 μ*M* pioglitazone was associated with a significant difference from the control, but was lower than that for 10 μ*M* (Av. 1.64, $p < 0.05$). The effect of 1 μ*M* pioglitazone was almost the same as the control (Av. 0.21). About 10 μ*M* was thus set as the optimal concentration of pioglitazone for adipogenesis of adipo-precursor cells. Next, pioglitazone was compared with IGF1 and IGF2. It is interesting to note that all levels of IGF2 were associated with very high levels of PPAR-γ mRNA (2 μ*M*: Av. 5.34; 20 μ*M*: Av. 9.16; 200 μ*M*: Av. 6.80). In the examination of the effect of IGF1 on the PPAR-γ mRNA level, 200 μ*M* was the only level to show a significant difference from the control (Av. 4.71, $p < 0.05$). About 10 μ*M* pioglitazone was associated with similar PPAR-γ mRNA expression to IGF1 and IGF2, which are known to be PPAR-γ inducers. These results indicated that 10 μ*M* pioglitazone is reasonable as the optimal level for inducing PPAR-γ mRNA expression.

This study was intended to aid the development of clinical applications, so 10 μ*M* pioglitazone was examined *in vivo*. Salmon collagen, as an injectable artificial biomaterial, was chosen here as it is clinically available and should work as a scaffold for adipose tissue by ligand protein interaction.[3–7] We think that the preferable size of collagen particles for scaffold of cell proliferation is between 70 μm and 130 μm in diameter, as the cells are between 10 μm and 20 μm in diameter. Our salmon collagen particles are, from our previous results, 223 μm or less in diameter on average. In terms of adjusting the salmon collagen, we chose 0.3–0.5% solution for the injectable component and included 10 μ*M* pioglitazone. This conditioned collagen with or without pioglitazone was implanted into mouse back under the skin layer and observed over time. At 1 week after implantation, both the collagen gels were observed without any immune elimination. A small number of fat droplets were observed at the edge of the collagen gel with pioglitazone. At 4 weeks after implantation, the collagen gel with pioglitazone was substituted by mature adipocytes in comparison with the case for the collagen gel without pioglitazone. We think that the source of mature adipocytes in collagen gels is migrated mesenchymal stem cells or migrated adipo-precursor cells and that the nourishment for adipocytes in collagen gels is from both peripheral vessels and indirect diffusion. These results are indicative of the possibility of promoting adipogenesis by collagen supplemented with pioglitazone as an adipose-inductive substance.

In future, if larger volumetric adipogenesis becomes a reality, this result should be highly promising for the following factors:

1. Soft tissue augmentation after tumor resection;
2. Prevention of wound contracture and promotion of wound healing;
3. Prevention of perforation, scar formation, and stenosis of intestinal mucosa damaged by digestive endoscopy; and
4. Esthetic improvement of poor form caused by body surface asperity.

## ACKNOWLEDGMENT

Authors thank Hatsumi Kobayashi and Masanobu Munekata (IHARA & Co., Ltd., Japan) for preparation of the salmon collagen with and without pioglitazone. The authors declare no conflicts of interest.

## REFERENCES

1. Youm YH, Yang H, Amin R, Smith SR, Leff T, Dixit VD. Thiazolidinedione treatment and constitutive-PPARγ activation induces ectopic adipogenesis and promotes age-related thymic involution. Aging Cell 2010;9:478–489.
2. Schadinger SE, Bucher NLR, Schreiber BM, Farmer SR. PPARγ2 regulates lipogenesis and lipid accumulation in steatotic hepatocytes. Am J Physiol Endocrinol Metab 2005;288: 1195–1205.

3. Yunoki S, Nagai N, Suzuki T, Munekata M. Novel biomaterial from reinforced salmon collagen gel prepared by fibril formation and cross-linking. J Biosci Bioeng 2004;98:40–47.
4. Nagai N, Kubota R, Okahashi R, Munekata M. Blood compatibility evaluation of elastic gelatin gel from salmon collagen. J Biosci Bioeng 2008;106:412–415.
5. Nagai N, Nakayama Y, Zhou YM, Takamizawa K, Mori K, Munekata M. Development of salmon collagen vascular graft: Mechanical and biological properties and preliminary implantation study. J Biomed Mater Res B Appl Biomater 2008;87:432–439.
6. Nagai N, Nakayama Y, Nishi S, Munekata M. Development of novel covered stents using salmon collagen. J Artif Organs 2009; 12:61–66.
7. Kawaguchi Y, Kondo E, Kitamura N, Arakaki K, Tanaka Y, Munekata M, Nagai N, Yasuda K. In vivo effects of isolated implantation of salmon-derived crosslinked atelocollagen sponge into an osteochondral defect. J Mater Sci Mater Med 2011;22:397–404.
8. Rosen ED, Walkey CJ, Puigserver P, Spiegelman BM. Transcriptional regulation of adipogenesis. Genes Dev 2000;14:1293–1307.
9. Kelly JL, Findlay MW, Knight K, Penington A, Thompson EW, Messina A, Morrison WA. Contact with existing adipose tissue is inductive for adipogenesis in matrigel. Tissue Eng 2006;12:2041–2047.
10. Findley MW, Messina A, Thompson EW, Morrison WA. Long-term persistence of tissue-engineered adipose flaps on a murine model to 1 year: An update. Plast Reconstr Surg 2009;124:1077–1084.
11. Phulpin B, Gangloff P, Tran N, Bravetti P, Merlin JL, Dolivet G. Rehabilitation of irradiated head and neck tissue by autologous fat transplantation. Plast Reconstr Surg 2009;123:1187–1197.
12. Kimura Y, Ozeki M, Inamoto T, Tabata Y. Adipose tissue engineering based on human preadipocytes combined with gelatin microspheres containing basic fibroblast growth factor. Biomaterials 2003;24:2513–2521.
13. Allan EH, Ho PW, Umezawa A, Hata J, Makishima F, Gillespie MT, Martin TJ. Differentiation potential of a mouse bone marrow stromal cell line. J Cell Biochem 2003;90:158–169.
14. Kern PA, Marshall S, Eckel RH. Regulation of lipoprotein lipase in primary cultures of isolated human adipocytes. J Clin Invest 1985; 75:199–208.
15. Bodles AM, Banga A, Rasouli N, Ono F, Kern PA, Owens RJ. Pioglitazone increases secretion of high-molecular-weight adiponectin from adipocytes. Am J Physiol Endocrinol Metab 2006;291:E1100–E1105.
16. Yamanouchi K, Ban A, Shibata S, Hosoyama T, Murakami Y, Nishihara M. Both PPARγ and C/EBPα are sufficient to induce transdifferentiation of goat fetal myoblasts into adipocytes. J Reprod Dev 2007;53:563–572.
17. Gurnell M. Peroxisome proliferator-activated receptor gamma and the regulation of adipocyte function: Lessons from human genetic studies. Best Pract Res Clin Endocrinol Metab 2005;19:501–523.
18. Higashi Y, Holder K, Delafontaine P. Thiazolidinediones upregulate insulin-like growth factor-1 receptor via a peroxisome proliferator-activated receptor gamma-independent pathway. J Biol Chem 2010;285:36361–36368.
19. Kleiman A, Keats EC, Chan NG, Khan ZA. Elevated IGF2 prevents leptin induction and terminal adipocyte differentiation in hemangioma stem cells. Exp Mol Pathol 2013;94:126–136.

Society For Biomaterials

# Development of tissue-engineered self-expandable aortic stent grafts (Bio stent grafts) using in-body tissue architecture technology in beagles

**Hidetake Kawajiri,[1,2] Takeshi Mizuno,[1] Takeshi Moriwaki,[1] Hatsue Ishibashi-Ueda,[3] Masashi Yamanami,[1,2] Keiichi Kanda,[2] Hitoshi Yaku,[2] Yasuhide Nakayama[1]**

[1]Division of Medical Engineering and Materials, National Cerebral and Cardiovascular Center Research Institute, Osaka, Japan
[2]Department of Cardiovascular Surgery, Kyoto Prefectural University of Medicine, Kyoto, Japan
[3]Department of Pathology, National Cerebral and Cardiovascular Center Research Institute, Osaka, Japan

Received 26 October 2013; revised 2 May 2014; accepted 17 May 2014
Published online 3 June 2014 in Wiley Online Library (wileyonlinelibrary.com). DOI: 10.1002/jbm.b.33218

**Abstract:** In this study, we aimed to describe the development of tissue-engineered self-expandable aortic stent grafts (Bio stent graft) using in-body tissue architecture technology in beagles and to determine its mechanical and histological properties. The preparation mold was assembled by insertion of an acryl rod (outer diameter, 8.6 mm; length, 40 mm) into a self-expanding nitinol stent (internal diameter, 9.0 mm; length, 35 mm). The molds ($n = 6$) were embedded into the subcutaneous pouches of three beagles for 4 weeks. After harvesting and removing each rod, the excessive fragile tissue connected around the molds was trimmed, and thus tubular autologous connective tissues with the stent were obtained for use as Bio stent grafts (outer diameter, approximately 9.3 mm in all molds). The stent strut was completely surrounded by the dense collagenous membrane (thickness, ~150 μm). The Bio stent graft luminal surface was extremely flat and smooth. The graft wall of the Bio stent graft possessed an elastic modulus that was almost two times higher than that of the native beagle abdominal aorta. This Bio stent graft is expected to exhibit excellent biocompatibility after being implanted in the aorta, which may reduce the risk of type 1 endoleaks or migration. © 2014 Wiley Periodicals, Inc. J Biomed Mater Res Part B: Appl Biomater, 103B: 381–386, 2015.

**Key Words:** endovascular aortic repair (EVAR), covered stents, connective tissue, in vivo tissue engineering, stent graft

**How to cite this article:** Kawajiri H, Mizuno T, Moriwaki T, Ishibashi-Ueda H, Yamanami M, Kanda K, Yaku H, Nakayama Y 2015. Development of tissue-engineered self-expandable aortic stent grafts (Bio stent grafts) using in-body tissue architecture technology in beagles. J Biomed Mater Res Part B 2015:103B:381–386.

## INTRODUCTION

Aortic aneurysms, which can be fatal in cases here they rupture, have been treated surgically using artificial grafts implanted via thoracotomy or laparotomy for several decades; however, the mortality rate of such procedures is high owing to their invasiveness and the frail nature of many patients.[1]

Endovascular aortic repair (EVAR) using a stent graft was first performed in humans by Parodi et al. in 1991.[2] Subsequently, endovascular repair of the aorta was first applied to the thoracic aorta (thoracic endovascular aortic repair; TEVAR) in 1994 by Dake et al.[3] TEVAR and EVAR have since become important treatment options for high-risk patients as they are associated with lower postoperative mortality and morbidity rates compared with open surgical aortic repair.[4–6] Although significant improvements have been made in implantation techniques and medical devices, late complications such as stent graft migration and endoleaks still occur and represent important issues that need to be rectified. Most of these complications are caused by an angulated or short landing zone[7,8]—which is the nonaneurysmal cylindrical part of the aorta that is used for stent graft fixation—and/or a lack of adaptation to late aortic remodeling; therefore, stent grafts with landing zones that completely adapt to the native aorta would be ideal. Based on our previous experience with the implantation of tissue-engineered materials, we consider that stent grafts constructed using tissue-engineered materials may be able to easily adapt to native vessels soon after implantation.[9,10]

We have developed autologous prosthetic tissues using the in-body tissue architecture technology, which is a novel and practical approach to regenerative medicine based on the tissue encapsulation of foreign materials in living bodies. Such in-body materials have been used to develop vascular grafts (Biotubes),[9] heart valves (Biovalves),[10] and

**Correspondence to:** Y. Nakayama (e-mail: ny@ncvc.go.jp)
Contract grant sponsor: Grant-in-Aid for Scientific Research; contract grant number: B23360374, B25293299, from the Ministry of Education, Culture, Sports, Science and Technology of Japan

materials for cardiac reconstruction. The in-body tissue architecture technology has the following advantages: (1) the prosthesis barely induces adverse immunological reactions, (2) the materials are biocompatible, (3) the prosthesis has the potential to grow with the recipient, and (4) the fabrication of such prostheses does not require *in vitro* cell management or clean laboratory facilities.

With regard to in-body tissue-engineered stent grafts, we have fabricated small-caliber (2 mm) balloon-expandable autologous tissue-covered stents in rabbits, which displayed excellent wall strength and were useful for various endovascular therapies.[11] In this study, we aimed to describe the development of tissue-engineered self-expandable aortic stent grafts (Bio stent grafts) using in-body tissue architecture technology in beagles and to determine its mechanical and histological properties.

## MATERIALS AND METHODS

### Preparation of the Bio stent graft

The experimental animals were beagles weighing 9.0–10.5 kg ($n = 3$). All the experimental animals received care according to the Principles of Laboratory Animal Care formulated by the National Institutes of Health (Publication No. 56-23, 1985), and the research protocol (No. 13034) was approved by the ethics committee of the National Cerebral and Cardiovascular Center Research Institute.

To determine the most appropriate size for the stent graft, the diameter of the beagle abdominal aorta was evaluated by aortography using a marker pigtail catheter, which was inserted into the aorta along a 0.035-in guidewire, and the software OsiriX (version 3.9; www.osirix-viewer.com), at 5 points located 10 mm apart from each other (Figure 1). The first point was located close to the origin of the lower renal artery. The calculated mean diameter of the beagle aorta was 7.7 ± 0.2 mm. The diameter of the Bio stent graft was fixed at 9.0 mm, which is 115% larger than the diameter of the native abdominal aorta.

A cylindrical acryl rod (outer diameter, 8.6 mm; length, 40 mm) produced by a three-dimensional printer (ProJet HD 3000, 3D Systems, Rock Hill, SC) and a self-expandable nitinol metal stent (Luminexx; diameter, 6 mm; length, 36 mm; BARD, Karlsruhe, Germany, and rememorized to an internal diameter of 9 mm by Piolax Medical Services, Yokohama, Japan) were combined to assemble a mold for the Bio stent graft [Figure 2(A)]. Dorsal subcutaneous pouches were created in three beagles using blunt scissors, and the molds ($n = 6$, two per beagle) were inserted into each pouch under anesthesia induced by the intramuscular injection of ketamine (20 mg/kg) and maintained by the intravenous injection of sodium pentobarbital (20 mg/kg) [Figure 2(B)]. After 4 weeks, the molds, covered with connective tissue, were harvested. The six Bio stent grafts were obtained after trimming the redundant fragile tissue and removing the acryl rods. One of these grafts was used for the histopathological examination, and the rest were used to measure the mechanical properties.

### Mechanical properties of the Bio stent graft

The tensile strength of the Bio stent graft ($n = 4$) was measured using a tensile strength machine (P&M, Fukushima, Japan). As specimens, the graft wall, which covered the stent struts, was cut in size of 10 mm × 10 mm. The specimens after fixation to the sample folder were stress-loaded to rupture at a rate of 0.05 mm/s at the direction without disturbing by the stent strut and maximum elastic modulus was determined as the maximum slope of the linear section of the stress–strain curve. For use as controls, tubular connective tissues (10 mm × 10 mm) without stents (Biotube; internal diameter, 8.6 mm; $n = 4$) were prepared similarly by using the same cylindrical acryl rod (outer diameter, 8.6 mm) mentioned above and cutting. The robustness of the Bio stent graft ($n = 1$) was evaluated by repeatedly shrinking the graft to 2 mm and releasing the pressure (reverting it to the original diameter) for several times using a crimping device.

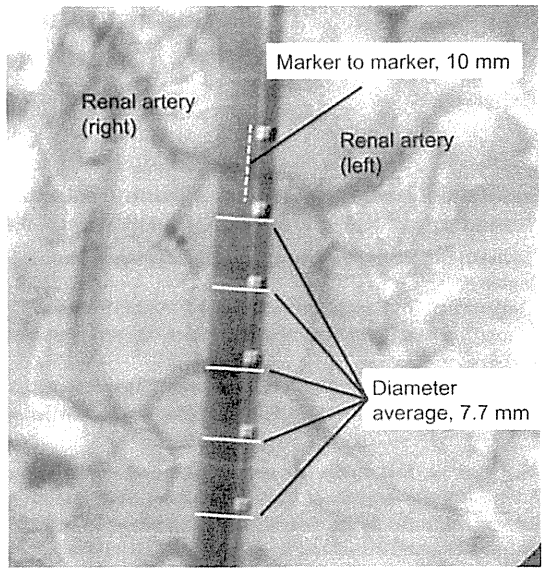


FIGURE 1. Aortography was performed using a marker pigtail catheter inserted via the femoral artery. The mean diameter of the abdominal aorta (7.7 mm in the infrarenal region) was calculated using OsiriX software. [Color figure can be viewed in the online issue, which is available at wileyonlinelibrary.com.]

### Histological examination

The Bio stent graft was fixed with 10% of formaldehyde in phosphate-buffered solution for 48 h, embedded in paraffin, and examined with light microscopy. Circumferential cross-sections of the Bio stent graft were prepared and subjected to hematoxylin–eosin, Elastica van Gieson, and Masson's trichrome staining, which were performed according to the standard procedures.

### Statistical analysis

The results are expressed as mean ± standard error of the mean. Comparisons were performed with an unpaired *t*-test (Student's *t*-test).

## RESULTS

### Fabrication of the Bio stent grafts

Four weeks after they were embedded into the subcutaneous pouches of the beagles [Figure 2(B)], we noted that the

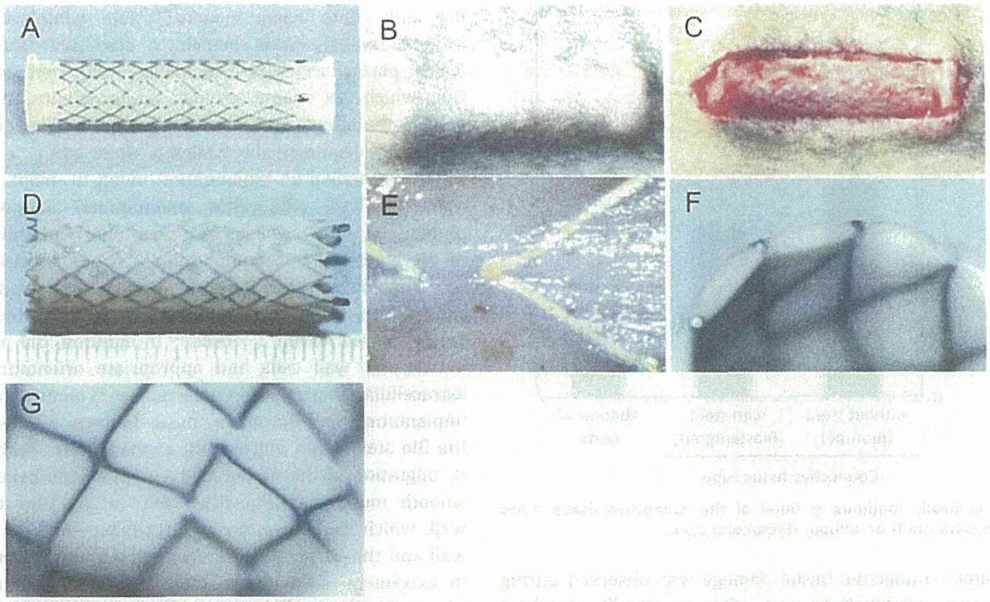


**FIGURE 2.** (A) The mold for the Bio stent graft prepared by assembly of a self-expandable stent (inner diameter, 9.0 mm) and a cylindrical acryl rod (outer diameter, 8.6 mm; length, 40 mm). (B) The mold embedded into the dorsal subcutaneous pouch of the beagle. (C) After 4 weeks, the mold was completely covered with connective tissue. (D) The Bio stent graft obtained after trimming the redundant fragile tissue around the mold. (E) The outer surface of the Bio stent graft fully covered with thin, smooth, and almost transparent connective tissue membrane. (F) The stent strut completely impregnated into the Bio stent graft wall. (G) The smooth and flat luminal surface of the Bio stent graft. [Color figure can be viewed in the online issue, which is available at wileyonlinelibrary.com.]

preparation molds [Figure 2(A)] assembled with acryl rods and stents were completely encapsulated by connective tissue and exhibited marked neovascularization [Figure 2(C)]. The molds capsulated completely with connective tissue could be easily harvested from the pouches by stripping the surrounding loose tissue. After trimming the redundant fragile tissue from the molds, and removing the acryl rods, the tissue-covered self-expandable stent grafts were obtained for use as Bio stent grafts [Figure 2(D)].

The outer surface of the Bio stent graft was completely covered with a thin, smooth, and almost transparent connective tissue membrane [Figure 2(E)]. The stent and tubular connective tissue was directly contacted [Figure 2(F)]. The stent strut was completely impregnated into the wall [Figure 3(A,B)]. The luminal surface was also smooth and flat [Figure 2(G)], and no projection of the stent strut was noted [Figure 3(A,B)]. The graft wall thickness was almost homogeneous, and was approximately 150 μm (height of the stent strut, 90 μm; strut to the inner surface, 35 μm; strut to outer surface, 25 μm). Around the stent struts, some cells including foreign body giant cells and macrophages were present [Figure 3(B)]. The graft wall was mainly composed of collagen [Figure 3(C)] and no elastic fibers were present [Figure 3(D)].

### Mechanical properties of the Bio stent grafts

The elastic modulus of the Bio stent grafts was 2203 ± 163 kPa, which was similar to the elastic modulus of the connective tissue tubes without stents (Biotubes) that were used as controls (Figure 4). Additionally, the elastic modulus of the Bio stent graft was almost twice as high as that of the native beagle abdominal aorta (1267 ± 690 kPa).

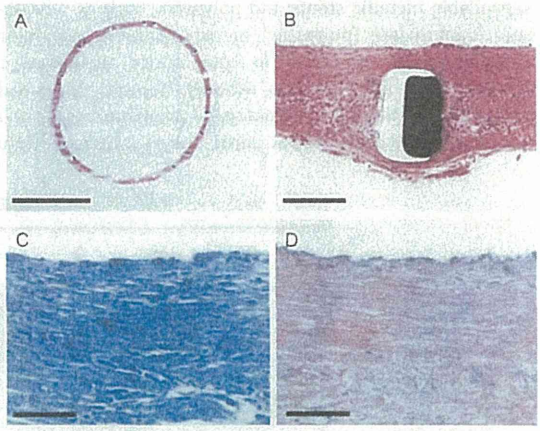


**FIGURE 3.** (A) Histological images of the whole circumferential cross-section of the Bio stent graft stained with standard hematoxylin–eosin. (B) The stent struts completely embedded within the connective tissue (thickness, ~150 μm), stained with hematoxylin–eosin. (C) Rich and dense collagen fibers (stained in blue) were present in Masson's trichrome staining. (D) No elastic fibers were seen in Elastica van Gieson staining. Scale bars: A: 5 mm; B: 100 μm; C,D: 25 μm. [Color figure can be viewed in the online issue, which is available at wileyonlinelibrary.com.]

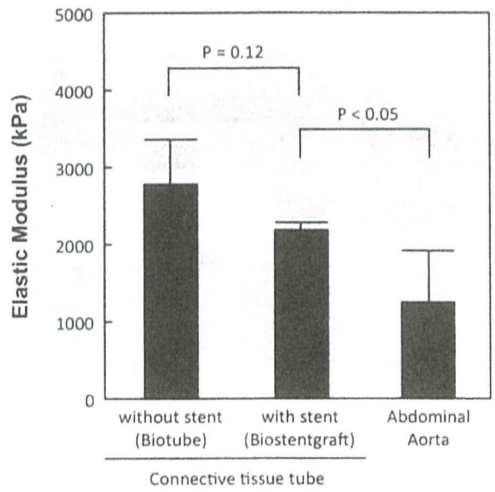


FIGURE 4. Elastic modulus at burst of the connective tissue tubes with (Bio stent graft) or without (Biotube) a stent.

Minimal connective tissue damage was observed during macroscopic examination, even after repeatedly shrinking the Bio stent graft to 2 mm and releasing the pressure (reverting it to the original diameter of 9 mm) with a crimping device (Figure 5). Therefore, the Bio stent graft could be placed in a 10-Fr sheath without damage. The stent strut was shrunk with the tissue membrane. The strut did not jump out of the membrane during crimping. The connection between the stent and the connective tissue membrane was extremely robust.

## DISCUSSION

Aortic stent grafts constructed using a combination of self-expandable metallic stents and polymers, such as polyethylene terephthalate (polyester) or expanded polytetrafluoroethylene, have been used to treat aortic aneurysms for decades, and their use has recently become more widespread.[12,13] Although commercially available stent grafts have been shown to prevent aortic aneurysms from rupturing and other aortic events,[5,6] late complications that require reintervention remain a significant issue. Endoleaks—particularly type 1 endoleaks—and stent graft migration, which are related to poor conformability of the stent graft to the native aorta, are the major complications associated with commercially available stent grafts. A previous report on endograft explantation owing to major complications of EVAR noted little endoluminal incorporation in most cases, which was suggestive of poor neointimal growth in the stent graft's landing zone.[14] In our experience with the implantation of Biotube vascular grafts into beagle carotid arteries, excellent endothelialization of the Biotubes was observed within 2 weeks.[15] In addition, the production of vascular wall cells and appropriate orientation of the extracellular matrix were detected at 3 months after graft implantation.[15,16] Based on these findings, we believe that the Bio stent graft will exhibit similar *in vivo* findings—that is, migration of the native cells such as endothelial cells or smooth muscle actin-positive cells to the Bio stent graft wall, which leads to a strong attachment between the graft wall and the aorta. Such *in vivo* adaptation may not be seen in extremely early phase after implantation, though if it occurs in the landing zone of the stent graft in several weeks, it would be possible to achieve tighter graft fixation and long-term excellent conformability even in angulated or short landing zones. In addition, early endothelialization has great benefits in terms of the antithrombogenicity of Bio stent grafts and Biotubes. Regarding the *in vivo* stent graft behavior, stent strut would not fall of from surrounding tissue toward the luminal direction, because of the strong adhesion, and the presence of intra-aortic pressure. However, there may be a risk of stent movement toward the outer direction if the radial force of the stent overwhelms the strength of adhesion between stent and connective tissue.

Another expected benefit of the Bio stent graft is the tolerance to bacterial infection. Artificial graft infections, which are mainly associated with polyester grafts, often lead to fatal complications such as the formation of an aortoenteric fistula or pseudoaneurysm.[17–20] To manage these complications,

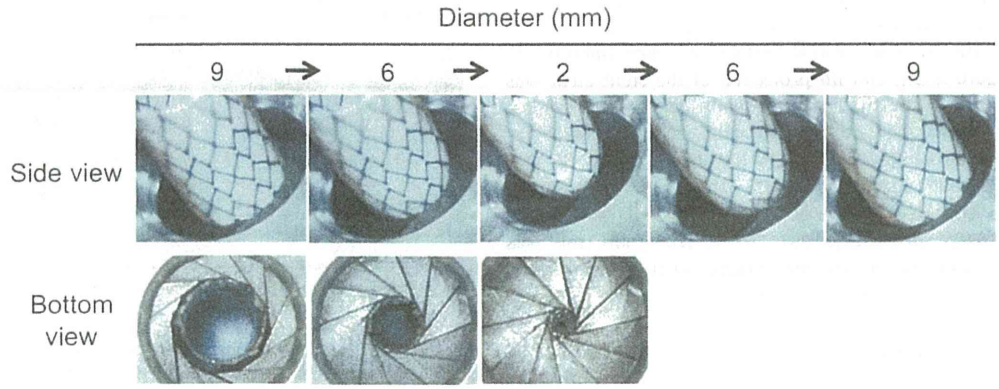


FIGURE 5. The robustness test of the Bio stent graft by repeatedly shrinking the graft to 2 mm and releasing the pressure (reverting it to the original diameter of 9 mm) by a crimping device. [Color figure can be viewed in the online issue, which is available at wileyonlinelibrary.com.]

homograft replacement with an omentum flap can be applied; however, despite a great amount of effort being expended, the outcomes are often not satisfactory.[17] In addition, the number of potential homografts is limited, and suitable replacements are not always available from tissue banks. The palliative covering of fistulas with ready-made endovascular stent grafts has also been reported although the frequency of recurrent infections among such cases is extremely high.[17,18] Thus, the Bio stent graft, which is covered by connective tissue, may be useful for the primary management of graft infections or aortoenteric fistulas.

In this study, we developed an autologous tissue-covered stent graft using in-body tissue architecture technology. As described previously, the greatest benefit of this technology is that it is possible to develop tissue-engineered stent grafts without complex *in vitro* cell management techniques or clean laboratory facilities, which are expensive and labor intensive. Another benefit of this technology is that it allows stent grafts to be constructed "*en bloc*"; therefore, it is not necessary to place an attachment suture between the metal stent and the graft fabric, which is technically demanding and time consuming. It is more difficult to fabricate tissue-covered stents utilizing the cell seeding technique as reported previously.[21] In this study, as the metal stent is completely and tightly embedded in connective tissue, it has a low profile. The ratio of the expanded diameter to the minimum compressed diameter was 4.5 (outer diameter ratio, 9.0 mm:2.0 mm), which would allow the Bio stent graft to be inserted via the femoral artery in beagles. Waiting for 4–6 weeks for fabricating the Bio stent graft would not be appropriate in some clinical settings, such as emergency cases. Though in elective cases, aortic aneurysm repair is planned several months later after the aneurysm is considered as an indication for treatment. If there is no rapid expansion in the landing zone, we think it may be possible to embed the appropriate sized molds and wait for 4–6 weeks.

In this study, the Bio stent graft was designed to cover a beagle's infrarenal abdominal aorta (mean diameter, 7.7 mm; length, 60 mm). The fabricated Bio stent graft had an outer diameter of 9.0 mm, which is 115% larger than that of the native aorta. Hayashida et al.[22] examined the relationship between the thickness of a fabricated biovalve leaflet and the internal diameter of the scaffold used to produce it, and reported that a scaffold with a larger internal diameter (20 mm) produced thicker leaflet tissue than a scaffold with a smaller internal diameter (5 mm). The mechanical properties of the leaflets also reflected the thickness of the tissue. Based on the abovementioned findings, we consider that it would be possible to obtain stronger and thicker biomaterials by implanting a larger scaffold. Thus, we could fabricate stronger aortic stent grafts for use in the thoracic aorta or transcatheter valve implantation by implanting larger rods.

We have demonstrated the functionality and excellent durability of *in vivo* tissue-engineered vascular grafts (Biotubes)[16] and valves (Biovalves)[23] under high-pressure systemic flow. As shown in Figure 3, the wall of the Bio stent graft produced in this study exhibited approximately 80% of the tensile strength displayed by a Biotube of the same diameter. The definite reason why the Bio stent graft has a lower elastic modulus than the Biotube is not clearly clarified. We think this might have been owing to the differences in connective tissue formation around the molds during the 4-week graft production period, and the presence of the stent strut may influence the composition or density of connective tissue. However, the Bio stent graft possessed an elastic modulus that was almost twice as high as that of the native beagle abdominal aorta, and hence we consider that this Bio stent graft would enable the exclusion of aortic aneurysms without disrupting the graft wall in beagles.

## CONCLUSIONS

We developed a self-expanding large-caliber stent graft covered with autologous membranous tissues (Bio stent graft) using in-body tissue architecture technology. The connection between the stent and the connective tissue membrane was extremely robust. This Bio stent graft is expected to exhibit excellent biocompatibility after being implanted in the aorta, which may reduce the risk of type 1 endoleaks or migration. As we noted that the Bio stent graft could shrink to 2 mm with little damage, our next study will examine the implantation of Bio stent grafts in animal aortas to confirm their conformability and biocompatibility with the native aorta.

## ACKNOWLEDGMENT

The authors thank Mr. Yasuhiro Hoshi and Ms. Manami Sone for their technical support in this study.

## REFERENCES

1. Knepper J, Upchurch GR. A review of clinical trials and registries in descending thoracic aortic aneurysms. Semin Vasc Surg 2010; 23:170–175.
2. Parodi JC, Palmaz JC, Barone HD. Transfemoral intraluminal graft implantation for abdominal aortic aneurysms. Ann Vasc Surg 1991;5:491–499.
3. Dake MD, Miller DC, Semba CP, Mitchell RJ, Walker PJ, Liddell RP. Transluminal placement of endovascular stent-grafts for the treatment of descending thoracic aortic aneurysms. N Engl J Med 1994;331:1729–1734.
4. Garcia-Toca M, Eskandari MK. Regulatory TEVAR clinical trials. J Vasc Surg 2010;52:22S–25S.
5. United Kingdom EVAR Trial Investigators, Greenhalgh RM, Brown LC, Powell JT, Thompson SG, Epstein D, Sculpher MJ. Endovascular versus open repair of abdominal aortic aneurysm. N Engl J Med 2010;362:1863–1871.
6. Prinssen M, Buskens E, Blankensteijn JD, DREAM trial participants. Quality of life endovascular and open AAA repair. Results of a randomized trial. Eur J Vasc Endovasc Surg 2004;27: 121–127.
7. Torsello G, Troisi N, Donas KP, Austermann M. Evaluation of the Endurant stent graft under instructions for use vs. off-label conditions for endovascular aortic aneurysm repair. J Vasc Surg 2011; 54:300–306.
8. Hoshina K, Kato M, Hosaka A, Miyahara T, Mikuriya A, Ohkubo N, Miyata T. Middle-term results of endovascular aneurysm repair in Japan: Does intraoerative endovascular management against the hostile aneurismal neck prevent the proximal type I endoleak? Int Angiol 2011;30:467–473.
9. Nakayama Y, Ishibashi-Ueda H, and Takamizawa K. In vivo tissue-engineered small-caliver arterial graft prosthesis consisting of autologous tissue (biotube). Cell Transplant 2004;13:439–449.
10. Yamanami M, Yahata Y, Uechi M, Fujiwara M, Ishibashi-Ueda H, Kanda K, Watanabe T, Tajikawa T, Ohba K, Yaku H, Nakayama Y. Development of a completely autologous valved conduit with the

sinus of valsalva using in-body tissue architecture technology: A pilot study in pulmonary valve replacement in a beagle model. Circulation 2010;122:S100–S106.
11. Nakayama Y, Zhou YM, Ueda-Ishibashi H. Development of in vivo tissue-engineered autologous tissue-covered stents (biocovered stents). J Artif Organs 2007;10:171–176.
12. D'Elia P, Tyrrell M, Azzaoui R, Sobocinski J, Koussa M, Valenti D, Haulon S. Zenith abdominal aortic aneurysm endovascular graft: A literature review. J Cardiovasc Surg 2009;50:165–170.
13. Sayeed S, Marone LK, Makaroun MS. The Gore Excluder endograft device for the treatment of abdominal aortic aneurysms. J Cardiovasc Surg 2006;47:251–260.
14. Brinster CJ, Fairman RM, Woo EY, Wang GJ, Carpentier JP, Jackson BM. Late open conversion and explantation of abdominal aortic stent grafts. J Vasc Surg 2011;54:42–47.
15. Watanabe T, Huang H, Hayashida K, Okamoto Y, Nemoto Y, Kanda K, Yaku H, Nakayaka Y. Development of small-caliber biotube vascular grafts: Preliminary animal implantation study. Artif Organs 2005;29:733.
16. Watanabe T, Kanda K, Yamanami M, Ishibashi-Ueda H, Yaku H, Nakayama Y. Long-term animal implantation study of biotube-autologous small-caliver vascular graft fabricated by in-body tissue architecture. J Biomed Mater Res B Appl Biomater 2011;1: 120–126.
17. Chenu C, Marcheix B, Barcelo C, Rousseau H. Aorto-enteric fistula after endovascular abdominal aortic aneurysm repair: Case report and review. Eur J Vasc Endovasc Surg 2009;37:401–406.
18. Danneels MIL, Verhagen HJM, Teijink JAW, Cuypers P, Nevelsteen A, Vermassen FEG. Endovascular repair for aortoenteric fistula: A bridge too far or a bridge to surgery. Eur J Vasc Endovasc Surg 2006;32:27–33.
19. Fatima J, Duncan AA, de Grandis E, Oderich GS, Kalra M, Gloviczki P, Bower TC. Treatment strategies and outcomes in patients with infected aortic endografts. J Vasc Surg 2013;58:371–379.
20. Kubota S, Shiiya N, Shingu Y, Wakasa S, Ooka T, Tachibana T, Yamauchi H, Ishibashi Y, Oba JI, Matsui Y. Surgical strategy for aortoesophageal fistula in the endovascular era. Gen Thorac Cardiovasc Surg 2013;61:560–564.
21. Shin'oka T, Matsumura G, Hibino N, Naito Y, Watanabe M, Konuma T, Sakamoto T, Nagatsu M, Kurosawa H. Midterm clinical result of tissue-engineered vascular autografts seeded with autologous bone marrow cells. J Thorac Cardiovasc Surg 2005; 129:1330–1338.
22. Hayashida K, Kanda K, Yaku H, Ando J, Nayakaya Y. Development of an in vivo tissue-engineered autologous heart valve (the biovalve): Preparation of a prototype model. J Thorac Cardiovasc Surg 2007;134:152–159.
23. Takewa Y, Yamanami M, Kishimoto Y, Arakawa M, Kanda K, Matsui Y, Oie T, Ishibashi-Ueda H, Tajikawa T, Ohba K, Yaku H, Taenaka Y, Tatsumi E, Nakayama Y. In vivo evaluation of an in-body, tissue-engineered, completely autologous valved conduit (biovalve type VI) as an aortic valve in a goat model. J Artif Organs 2012;16:176–184.

JOURNAL OF TISSUE ENGINEERING AND REGENERATIVE MEDICINE
*J Tissue Eng Regen Med* (2013)
Published online in Wiley Online Library (wileyonlinelibrary.com) DOI: 10.1002/term.1859

RESEARCH ARTICLE

# In-body tissue-engineered collagenous connective tissue membranes (BIOSHEETs) for potential corneal stromal substitution

Naoaki Takiyama[1], Takeshi Mizuno[1,2], Ryosuke Iwai[2], Masami Uechi[1,2] and Yasuhide Nakayama[2]*
[1]*Department of Veterinary Medicine, College of Bioresource Sciences, Nihon University, Kanagawa, Japan*
[2]*Division of Medical Engineering and Materials, National Cerebral and Cardiovascular Centre Research Institute, Osaka, Japan*

## Abstract

**There is a severe shortage of donor cornea for transplantation in many countries. Collagenous connective tissue membranes, named BIOSHEETs, grown *in vivo* were successfully implanted in rabbit corneal stroma for *in vivo* evaluation of their suitability as a corneal stromal substitute to solve this global donor shortage. BIOSHEETs were prepared by embedding silicone moulds into dorsal subcutaneous pouches in rabbits for 1 month and stored in glycerol. After re-swelling in saline and trephining, disk-shaped BIOSHEETs (4 mm diameter) were allogeneically implanted into stromal pockets prepared in the right cornea of seven rabbits. Clinical tests for corneal thickness and transparency, and tissue analyses were performed. Because the BIOSHEETs (thickness, 131 ± 14 μm) obtained were opaque immediately after implantation, the transparency of the cornea decreased. The total thickness of the BIOSHEET-implanted cornea increased from 364 ± 21.0 μm to 726 ± 131 μm. After 4 weeks' implantation, the thickness of the cornea stabilized (493 ± 80 μm at 4 weeks and 447 ± 46 μm at 8 weeks). The transparency of the cornea increased progressively with time of implantation. The random orientation of collagen fibrils in the original BIOSHEETs tended to be homogeneous, similar to that of the native stroma. No inflammatory cells accumulated and fibroblast-like cells infiltrated the implant. The BIOSHEETs showed high biocompatibility with stromal tissues; however, further studies are needed to test its functional aspects. Although this research is only intended as a proof of concept, BIOSHEETs may be considered a feasible corneal stromal replacement, especially for treating visual impairment caused by stromal haze.**


**Received 28 March 2013; Revised 7 September 2013; Accepted 10 November 2013**

**Keywords** biocompatibility; connective tissue; cornea; implantation; tissue engineering

## 1. Introduction

The cornea is the transparent outer window to the eye and is one of the major refractive elements of the eye. The corneal stroma, which is a collagenous hydrogel with lesser amounts of glycosaminoglycans (proteoglycans that contains keratocytes) is sandwiched by non-keratinizing epithelium and inner single-layered endothelium. The corneal stroma comprises 90% of the thickness of the cornea and consists of regularly packed collagen fibrils arranged as orthogonal layers or lamellae. Approximately 70% of the dry weight of the corneal stroma is composed of collagen type I. The collagen fibrils of this tissue are regularly spaced, similar in diameter and run parallel to one another within lamellae. The transparency of the corneal stroma is attributed to the unique tight packing and uniform diameter of the collagen fibrils, which minimizes light scattering (Robert *et al.*, 2001; Knupp *et al.*, 2009; Hassell and Birk, 2010).

Corneal disorders that disrupt the uniformity of the stromal structure result in a loss of corneal transparency. Corneal disease is a major cause of blindness or severely impaired vision and affects more than 10 million people worldwide. In some parts of Africa and Asia the

* *Correspondence to: Yasuhide Nakayama, Division of Medical Engineering and Materials, National Cerebral and Cardiovascular Centre Research Institute, 5-7-1 Fujishirodai, Suita, Osaka 565–8565, Japan. E-mail: nakayama@ncvc.go.jp*

incidence of childhood cornea-related visual loss is 20 times higher than that in industrialized countries (Schwartz *et al.*, 1997; Whitcher *et al.*, 2001, 2002). Blindness caused by corneal disease is usually permanent. The only widely accepted treatment for corneal blindness is corneal transplantation.

However, there is a severe shortage of acceptable corneal tissue for transplantation, especially with the increase in the aging population and incidence of transmissible disease. Corneal transplantation has many limitations, including a lack of eye banking infrastructure and excessive cost, particularly in the Third World and developing countries (Feilmeier *et al.*, 2010). In addition, in so-called 'high-risk cases' where the recipient corneal bed is inflamed and/or neo-vascularized, the prognosis is poor and the graft failure rate is high (Streilein *et al.*, 1999; Williams and Coster, 2007; Chong and Dana, 2008).

Many groups have attempted to construct corneal substitutes. Various compounds have been used in corneal research, including synthetic materials such as silicone rubber, polymethylmethacrylate (PMMA), poly (2-hydroxyethyl methacrylate) or naturally occurring polymers such as collagen and hyaluronic acid, collagen-glycosaminogycan-chitosan and silk fibroin (Crawford *et al.*, 1993; Doane *et al.*, 1996; Lee *et al.*, 1996; Vijayasekaran *et al.*, 1997; Chen *et al.*, 2005; Builles *et al.*, 2007; Bray *et al.*, 2011). However, biological integration with the surrounding recipient tissue is still a major problem, and restoration of sensory or physiological corneal function has not been achieved. Alternatively, many groups have attempted to develop tissue-engineered corneal equivalents (Liu *et al.*, 2007; Fagerholm *et al.*, 2009, 2010; Merrett *et al.*, 2009; Duncan *et al.*, 2010; Tanaka *et al.*, 2011; Xiao *et al.*, 2011; Yoeruek *et al.*, 2011). An ideal scaffold for a tissue-engineered corneal equivalent should be biocompatible, non-immunogenic, non-mutagenic, sufficiently strong to withstand surgical procedures and optically clear (Feinberg, 2012). Therefore, the primary goal of this study was to prepare unique collagenous membranes (hereafter termed BIOSHEETs) for corneal stroma substitution by in-body tissue engineering (Nakayama *et al.*, 2004; Watanabe *et al.*, 2011; Hayashida *et al.*, 2007; Yamanami *et al.*, 2010). In this study, BIOSHEETs were prepared using in-body tissue engineering and transplanted into rabbit corneal stroma. The aim was to evaluate the biocompatibility, the transparency and the possibility of the BIOSHEETs as a potential corneal stroma substitution material *in vivo*.

# 2. Materials and methods

## 2.1. Animal studies

Studies were performed in accordance with the National Institutes of Health (NIH) guidelines for the care and use of laboratory animals' (National Institutes of Health 1996) and the Association for Research in Vision and Ophthalmology (ARVO) statement for the use of animals in ophthalmic and vision research under a protocol approved by the National Cerebral and Cardiovascular Center Research Institute Committee (No. 12002).

## 2.2. BIOSHEET preparation protocol

The mould for BIOSHEETs (Figure 1a) was prepared by terminal adhesion of silicone tubes (60 mm long, 20 mm diameter, 2 mm thick). Six Japanese white rabbits (2.7–3.0 kg) were given general anesthesia using a mixture of ketamine (50 mg/kg Ketalar; Daiichi Sankyo, Tokyo, Japan) and xylazine (5 mg/kg Selactar; Bayer Health Care, Tokyo, Japan) and maintained by bolus intramuscular injection of a quarter of the initial dose. A 5 cm incision was made at dorsal skin between last rib and ilium, and two moulds were placed into each subcutaneous pouch (Figure 1b), each incision was then sutured with 4–0 nylon (Figure 1c). The rabbits received 5 mg/kg systemic enrofloxacin (Baytril injectable; Bayer, Tokyo, Japan) for 1 week. After complete encapsulation of the moulds by connective tissue (i.e. 1 month after implantation) the implants were harvested (Figure 1d). The membranous tissue that formed as a BIOSHEET around the mould was obtained by trimming to remove fragile and redundant tissue adhered to the BIOSHEET tissue (Figure 1e). The BIOSHEETs were preserved by soaking in sterile pure glycerol (Wako Pure Chemical, Osaka, Japan), which is used clinically to preserve donor corneas for corneal transplantation in the developing world, at 4 °C for 1 week. Before implantation, BIOSHEETs were submerged in sterile physiological saline to allow irrigation for 10 min (Figure 1f).

## 2.3. BIOSHEET implantation procedure

The BIOSHEETs were implanted as an allogenic stromal substitute into the right cornea of seven Japanese white rabbits (2.8–3.0 kg). Rabbits were anesthetized with medetomidine (0.1 mg/kg Dorbene; Kyoritsu Seiyaku, Tokyo, Japan), butorphanol (0.2 mg/kg Vetorfal; Meiji Seika Pharma, Tokyo, Japan) and ketamine (25 mg/kg Ketalar; Daiichi Sankyo). In addition, oxybuprocaine hydrochloride (Benoxil ophthalmic solution 0.4%; Santen Seiyaku, Osaka, Japan) was given twice before surgery for induction of local anaesthesia. A 6-mm long incision with a depth approximately half that of the cornea was made at the dorsal limbus, and a stromal pocket was created using a scleral knife. A BIOSHEET was trephined to provide disks with a diameter of 4 mm (Figure 1h) and implanted into the pocket (Figure 1i). One of the six BIOSHEETs was used for transplantation to eliminate the potential confounding factor of biocompatibility. Control cornea received sham surgery

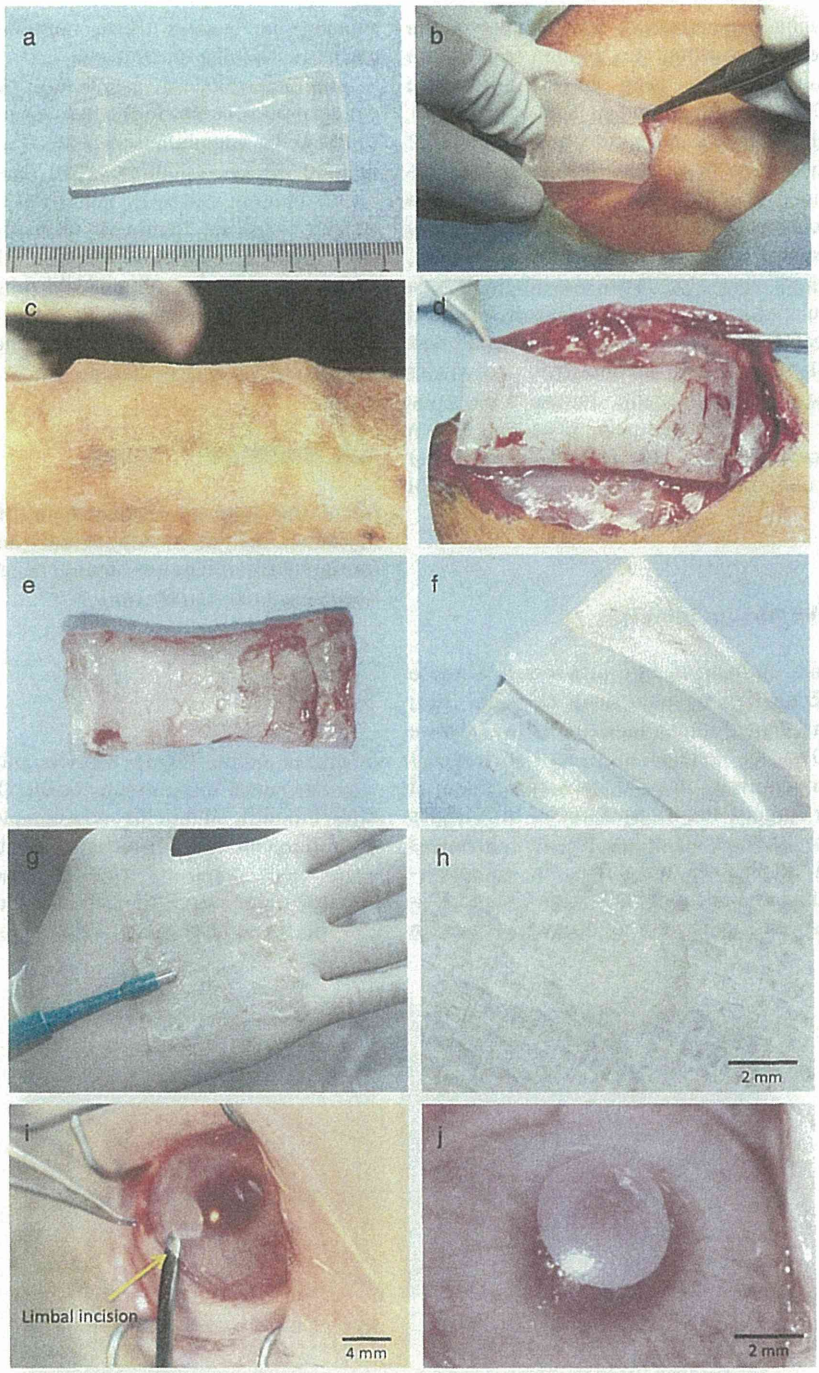


Figure 1. Preparation and implantation of BIOSHEET. (a) Silicone mould for BIOSHEET preparation. The mould at (b) and after (c) placing into the subcutaneous pouch; (d) The mould encapsulated completely with BIOSHEET tissue after 1 month of implantation; (e) BIOSHEET-covered mould after trimming to remove fragile and redundant tissue; (f,g) BIOSHEET preserved by soaking in sterile pure glycerol and submerged in physiological saline; (h) trephined BIOSHEET (4 mm in diameter); (i) implantation into stromal pocket of rabbit cornea; (j) immediately after implantation

($n = 4$). The incision was closed with one suture using 10–0 nylon, which was removed 2 weeks after surgery. After surgery, 5 mg/kg systemic enrofloxacin (Baytril injectable; Bayer) was administered daily for the first week. No immunosuppressive drugs were used.

## 2.4. Clinical test

Follow-up evaluations were performed daily on each rabbit for 7 days after surgery and then weekly. Corneal opacity grade, vascularization, corneal thickness and




DOI: 10.1002/term

corneal topography were assessed. Transparency of the cornea was assessed according to a grading scale where 0 indicated transparent by using surgical microscope (×10 ~ 20, OPMI pico; Alcon Japan, Tokyo, Japan), 1 indicated a slight haze that did not obscure the pupil, 2 indicated a moderate haze but distinguishable iris vessels and 3 indicated that the pupil and iris vessels were totally obscured. Corneal vascularization was graded on a scale of 0–4 where 0 = no vascularization, 1 = neovascularized area < ¼, 2 = neovascularized area ½, 3 = neovascularized area < ¾ and 4 = neovascularized area > ¾. Corneal thickness was measured at central part of implanted BIOSHEET with an ultrasonic pachymeter (AL-3000; Tomey, Nagoya, Japan). Corneal topography was measured using a topographic modelling system (TMS-4 Advanced; Tomey). Flat (Kf) and steep (Ks) meridians were derived from the measured topography of each cornea.

### 2.5. Qualitative tissue analyses

Two rabbits were euthanized by intravenous overdose (more than 75 mg/kg) of potassium chloride (KCl; Nichiiko, Toyama, Japan) under anaesthesia by a mixture of ketamine (50 mg/kg, Ketalar) and xylazine (5 mg/kg) at 4 weeks postoperatively; five rabbits were euthanized at 8 weeks after surgery. Pre-transplantation BIOSHEETs ($n = 2$) before and after soaking in glycerol and corneas implanted with BIOSHEETs were fixed in phosphate-buffered formalin and embedded in paraffin; 5-μm longitudinal sections were subjected to haematoxylin-eosin staining for general tissue morphology and Masson trichrome staining for collagen.

Immunohistological assay was performed for cell characterization. As antibodies, α-smooth muscle actin (α-SMA) for smooth muscle cells or myofibroblasts (1:50 dilution; Abcam, Cambridge, UK), vimentin for fibroblasts (1:50 dilution; Abcam), and RAM11 for macrophages (DAKO, Glostrup, Denmark) were used. After washing with phosphate-buffered saline (PBS), slides were incubated with Alexa Fluor®594 rabbit anti-mouse IgG antibody (1:200; Invitrogen, Carlsbad, CA, USA) and then incubated with 4′,6-diamidino-2-phenylindole (DAPI; Invitrogen) for nuclear staining.

### 2.6. Statistics

All of the data are expressed as the mean ± standard deviation. Analysis of variance and *t*-test were used to test for significant differences among the groups, and $p < 0.05$ was considered significant.

## 3. Results

A silicone mould (Figure 1a) was embedded in a subcutaneous pouch of six rabbits for BIOSHEET preparation. After 1 month, all moulds were completely encapsulated by autologous connective tissue membrane. The moulds were easily removed from the membranous tissue because there was little adhesion between the mould and the tissue (Figure 1f). The tissue obtained (i.e. the

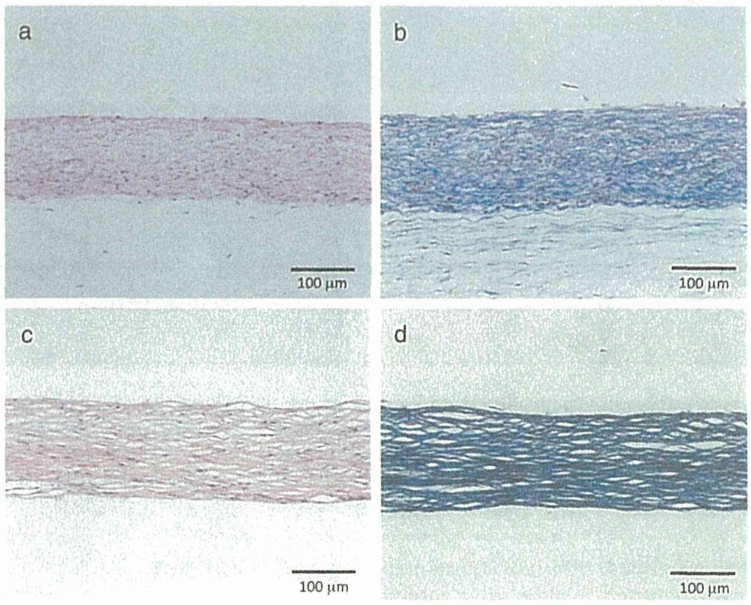


Figure 2. Haematoxylin and eosin section of BIOSHEETs before (a) and after (c) preservation in glycerine and submerged in physiological saline, and Masson's trichrome section of BIOSHEETs before (b) and after (d) preservation in glycerine and submerged in physiological saline




DOI: 10.1002/term

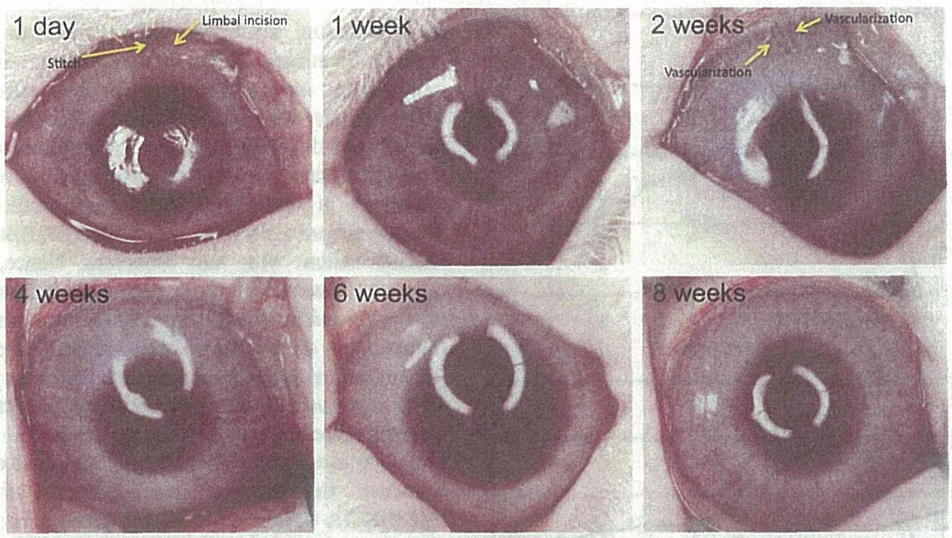


**Figure 3. Postoperative observation of BIOSHEET implanted into rabbit corneal stroma**

BIOSHEETs) comprised thin sheets with a smooth flat surface (6 × 6.5 cm, 131.0 ± 14.0 μm thick, Figure 1g). The success rate of BIOSHEET preparation was, therefore, 100%. However, it was opaque both before and after glycerol preservation (Figure 1h) with random orientation of the collagen fibres (Figure 2b,d). All cells in the BIOSHEET died after the it was immersed into glycerol for 1 week although many cell nuclei remained (Figure 2c).

All animals survived without infections or other complications during the follow-up period. Neo-vascularization, corneal thickness, corneal refractive power and histology were evaluated to investigate the possibility of the BIOSHEET as a corneal stromal substitution material. Slight corneal neovascularization that reached the corneal incision was noted up to 2 weeks postoperatively (Figure 3). The average corneal vascularized scores of BIOSHEET implanted corneas were 0.7 ± 0.5 at 1 week and 0.1 ± 0.4 at 2 weeks, which were almost same of those of sham-operated corneas (0.75 ± 1.0 at 1 week, 0.5 ± 1.0 at 2 weeks). At 4 weeks after implantation or sham operation all corneas had no neovascularization (scores 0). In addition, there was no inflammation or signs of rejection during implantation. Immediately after implantation, all BIOSHEET disks were opaque (Figure 1h). However, interestingly, each BIOSHEET became transparent over time in all rabbits (Figure 3). The transparency scores for the cornea after 4 weeks were significantly lower (1.7 ± 1.0 at 4 weeks and 0.6 ± 0.6 at 8 weeks) than those obtained immediately after implantation (3, $p < 0.05$) (Figure 4a). The transparency of the cornea increased progressively with time of implantation.

The total thickness of the cornea was 726.1 ± 131.0 μm immediately after implantation and almost the same even at 2 weeks after implantation (Figure 4b). The thickness was significantly greater than the pre-implantation thickness (364 ± 21.0 μm). Thickness markedly decreased in the first 4 weeks (493.0 ± 80.0 μm) and then remained stable until 8 weeks (447.0 ± 46.0 μm).

The increased postoperative corneal refractive power was attributed to the implanted BIOSHEETs and increased corneal thickness. After implantation, high refractive power (Figure 4c) and rough corneal topography remained (Figure 5).

The arrangement and orientation of the collagen lamellae of BIOSHEETs were heterogeneous at 4 weeks postoperatively, but they tended to take on a homogeneous character similar to that of the native corneal stroma at 8 weeks postoperatively (Figure 6). The boundaries of the BIOSHEETs were well defined at 4 weeks but became indistinct at 8 weeks. At 8 weeks after implantation fibroblast-like cells infiltrated into the implanted BIOSHEETs (Figure 7a), but there were no α-SMA positive cells (Figure 7b) or inflammatory cells (Figure 7c).

## 4. Discussion

The cornea is responsible for transmission and refraction of the light to the retina and for maintaining the shape of the eye. The cornea is an avascular and transparent tissue composed of three layers: the epithelium, stroma and endothelium. The extracellular matrix of the corneal stroma consists primarily of collagen type I with a lower amount of collagen type IV and proteoglycans (Knupp *et al.*, 2009; Hassell and Birk, 2010). Therefore, collagenous biomaterials such as collagen gels, and acellular porcine corneas are widely used as potential corneal substitutes (Liu *et al.*, 2007; Fagerholm *et al.*, 2009, 2010; Merrett *et al.*, 2009; Duncan *et al.*, 2010; Tanaka *et al.*, 2011; Xiao *et al.*, 2011; Yoeruek *et al.*, 2011). As alternative approach, autogenic transplantation of collagen-rich tissues such as ligaments,

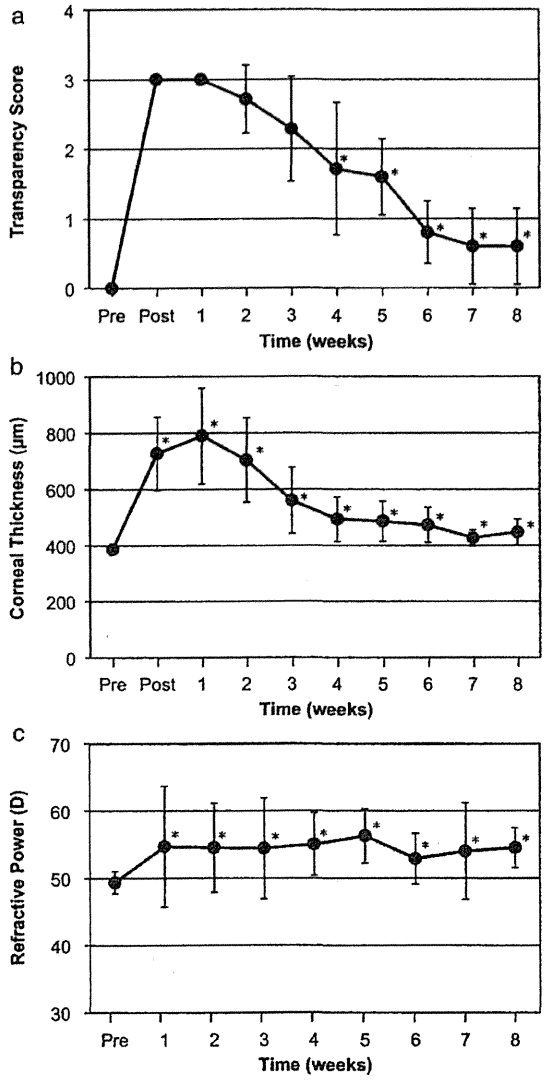


**Figure 4. (a) Mean values for corneal transparency. The corneas implanted with the BIOSHEET became hazy immediately after transplantation, but transparency was gradually restored. (b) Change in corneal thickness following implantation of BIOSHEETs into rabbit cornea. (c) Refractive power change following implantation of BIOSHEETs into rabbit cornea. Significant increase from preoperative values (*, $P < 0.05$)**

tendons, and skin have been widely applied for the replacement of damaged tissue (Jackson and Simon, 2002; Antonogiannakis *et al.*, 2005; de Vries Reilingh *et al.*, 2007; Carey *et al.*, 2009). However, there is no adequate autogenic tissue source (i.e. a tissue with high transparency and high mechanical strength) for substitution of the corneal stroma. Therefore, the primary goal of this study was to prepare collagenous membranes as BIOSHEETs for corneal stromal substitution. We evaluated the biocompatibility and transparency of BIOSHEETs transplanted into rabbit corneal stroma.

Biocompatibility factors, including cell compatibility, lack of immunogenicity, lack of toxicity and resistance to biodegradation, are critical for materials for tissue engineering (Feinberg 2012). In the present study, neovascularization, corneal thickness, corneal refractive power and histology were evaluated to investigate the biocompatibility of BIOSHEETs. Slight neovascularization of the corneal incision site was observed up to 2 weeks postoperatively in both BIOSHEETs implanted cornea and sham-operated cornea; however, BIOSHEET-induced neovascularization was not observed. Hence, neovascularization was considered to represent the wound healing of the corneal incision. The thickness of cornea increased immediately after surgery and gradually decreased; but did not return to the preimplantation thickness (Figure 4B). The increased postoperative corneal refractive powers are considered to result from the implanted BIOSHEETs and increased corneal thickness. Corneal topographies revealed the existence and location of implanted BIOSHEETs (Figure 5). Histologically, the BIOSHEET remained between stromal layers. The implanted BIOSHEET was infiltrated with corneal fibroblasts but not inflammatory cells. These results indicate that the BIOSHEET was well tolerated without inflammation, degradation or any signs of rejection, even though the implantation was allogeneic. Therefore, BIOSHEETs prepared using our technique appear to have excellent biocompatibility for corneal tissue.

This finding was expected based on our previous study of the implantation of cardiovascular tissues prepared similarly (Nakayama *et al.*, 2004; Hayashida *et al.*, 2007; Watanabe *et al.*, 2011; Yamanami *et al.*, 2010). BIOSHEETs mainly consist of collagen type I, which is the main biochemical component of the skin and corneal stroma (Knupp *et al.*, 2009; Hassell and Birk, 2010; Robert *et al.*, 2001). This similarity in composition between the native cornea and BIOSHEETs may underlie the high biocompatibility of BIOSHEETs implanted into the corneal stroma. The implanted BIOSHEETs were preserved in sterile pure glycerol, which is a simple, effective and economical preservation medium (King *et al.*, 1962; Sharma *et al.*, 2001). Glycerol-preserved tissue lacks antigenicity, which thus prevents graft rejection and obviates long-term immunosuppressive treatment (Chen *et al.*, 2010). Preservation in glycerol may have thus facilitated the engraftment of allogeneic BIOSHEETs into the rabbit cornea.

In this study, the original BIOSHEETs were opaque and obscured the pupil until several weeks after implantation; however, corneal transparency recovered progressively. The transparency of the normal cornea mainly depends on the architecture of the corneal stroma. Uniform collagen fibril diameter, uniform inter-fibrillar distance and orthogonal alignment of collagen fibres are necessary for corneal transparency (Knupp *et al.*, 2009; Hassell and Birk, 2010). Loss of transparency in the wounded cornea is caused by increased corneal thickness and increased diameter of collagen fibrils as well as poor fibrillar organization in the regenerated stroma (Quantock *et al.*, 1994). In this study, the corneas implanted with BIOSHEETs were thick and hazy immediately after implantation.